

920

STRESS-STRAIN CHARACTERISTICS AND HISTOLOGICAL STUDIES  
OF CANINE CONNECTIVE TISSUES



STRESS-STRAIN CHARACTERISTICS AND HISTOLOGICAL STUDIES  
OF CANINE CONNECTIVE TISSUES

By  
ABDUL LATIFF AHOOD

A Thesis  
Submitted to the School of Graduate Studies  
in Partial Fulfilment of the Requirements  
for the Degree  
Master of Engineering

McMaster University  
May 1978



To Mother  
"In Ever Loving Memory"



## ABSTRACT

This project is Part I of a study aimed at determining the stress-strain characteristics of various collagenous canine tissues, and relating them to their structure (histology). In addition Part II involves the isolation of the collagenous structures by enzymolysis of mucopolysaccharides and elastin, which results in the phenomenological elastic moduli of collagen in the various tissues.

The present study provides this through in vitro tensile experiments on various tissues from the dog in the native state, after elastin removal by enzymolysis, or after removal of collagen by autoclaving. The elastin component, which exhibits a linear stress-strain curve, determines the tensile modulus of the native tissue at low strain, while collagen determines the modulus at high strain. The removal of elastin significantly alters the moduli at low strain for most of the tissues, although the high-strain moduli remain essentially unchanged.



#### ACKNOWLEDGEMENTS

I would like to express my heartfelt gratitude to the following people whose help were highly instrumental in this work:

Dr. Y.F. Missirlis, my project supervisor, for his advice and guidance.

Frank Anderson and colleagues, and Dave Cragg for supplying me the various tissues.

Sharon Putns and colleagues for doing most of the histology work.

Drs. Cole and DeSa for lending me their microscope and camera facilities.

Mr. Ming Chong for the various enlightening discussions.

The Canadian Commonwealth Scholarship and Fellowship Administration for financing my program of studies.



## TABLE OF CONTENTS

	<u>Page Number</u>
TITLE PAGE.....	i
DEDICATION.....	ii
ABSTRACT.....	iii
ACKNOWLEDGEMENTS.....	iv
TABLE OF CONTENTS.....	v
LISTS OF TABLES AND FIGURES.....	vii
INTRODUCTION.....	1
1. Importance of Mechanical Study.....	1
2. Prior Work.....	3
3. Structure of the Various Tissues.....	9
4. Composition.....	13
MECHANICS OF TISSUES.....	15
1. Experimental Procedure.....	15
2. Results.....	18
3. Contribution of Individual Components.....	40
4. The Effect of Mucopolysaccharides (MPS) Removal.....	42
5. Explanation of Results.....	42
HISTOLOGY.....	45
HISTOLOGY OF STRAINED SAMPLE.....	54
DISCUSSION.....	60
SUMMARY OF CONCLUSIONS.....	68
REFERENCES.....	69



TABLE OF CONTENTS

	<u>Page Number</u>
APPENDIX 1 .....	73
APPENDIX 2 .....	81



## LIST OF TABLES AND FIGURES

<u>Figure #</u>	<u>Title</u>
1	Orientations of samples in descending aorta
2	Photographs of experimental set up
3	Typical stress-strain curves of dog's descending aorta (circumferential sample)
4	Typical stress-strain curves of dog's descending aorta (longitudinal sample)
5	Typical stress-strain curves of dog's ascending aorta (circumferential sample)
6	Typical stress-strain curves of dog's ascending aorta (longitudinal sample)
7	Typical stress-strain curves of dog's abdominal skin (longitudinal sample)
8	Typical stress-strain curves of dog's abdominal skin (transverse sample)
9	Typical stress-strain curves of dog's Achilles tendon
10	Typical stress-strain curves of dog's cornea
11	Schematic diagram of cornea showing equatorial and meridional section
12	Typical stress-strain curves of dog's sclera
13	Typical stress-strain curves of dog's ascending aorta (circumferential sample)
14	Typical stress-strain curves of dog's Achilles tendon
15	Typical stress-strain curves of dog's cornea
16	Histological micrograph of native descending aorta . Longitudinal section (Verhoeff)



<u>Figure #</u>	<u>Title</u>
17	Histological micrograph of native descending aorta. Circumferential section (Verhoeff)
18	Histological micrograph of native descending aorta. Longitudinal section (H&E)
19	Histological micrograph of native descending aorta. Circumferential section (H&E)
20	Histological micrograph of deelasinated descending aorta. Longitudinal section (Verhoeff)
21	Histological micrograph of deelasinated ascending aorta. Longitudinal section (Verhoeff)
22	Histological micrograph of native ascending aorta. Circumferential section (Verhoeff)
23	Histological micrograph of native ascending aorta. Longitudinal sample (Verhoeff)
24	Histological micrograph of native abdominal skin. Longitudinal section (Verhoeff)
25	Histological micrograph of deelasinated abdominal skin. Longitudinal section (Verhoeff)
26	Histological micrograph of deelasinated abdominal skin. Longitudinal section (Trichrome)
27	Histological micrograph of native Achilles tendon (Verhoeff)
28	Histological micrograph of native cornea (Verhoeff)
29	Histological micrograph of native sclera (Verhoeff)
30	Histological micrograph of strained ( $\epsilon = 80\%$ ) descending aorta
31	Histological micrograph of strained ( $\epsilon = 80\%$ ) abdominal skin.



<u>Figure #</u>	<u>Title</u>
32	Histological micrograph of strained ( $\epsilon = 150\%$ ) abdominal skin
33	Histological micrograph of strained ( $\epsilon = 2\%$ ) Achilles tendon
34	Histological micrograph of strained ( $\epsilon = 20\%$ ) cornea

<u>Table #</u>	<u>Title</u>
1	Variation in Modulus of Native and Deelastinated Descending Aorta
2	Variation in Modulus of Native and Deelastinated Ascending Aorta
3	Variation in Modulus of Native and Deelastinated Abdominal Skin
4	Variation in Modulus of Native and Deelastinated Achilles Tendon
5	Variation in Modulus of Native and Deelastinated Cornea
6	Variation in Modulus of Native and Deelastinated Sclera
7	Staining Methods Used in Histology of Dog's Tissues
8	Determination of "t" and "p" Values for the Dog's Descending Aorta



## INTRODUCTION

### 1. Importance of mechanical studies on various tissues

The aim of this project is to determine the stress-strain characteristics and the "elastic modulus" (see Appendix 1) of collagen from various tissues of the body and to show how the structural arrangement of the collagen fibres in these tissues is related to its mechanical properties.

This is Part I of the project dealing with the measurement of the stress-strain characteristics and the histology of the tissues.

Part II deals with the measurements and calculations of the induced porosity in the tissues by a collagen isolation technique and thus correcting the stress-strain curves.

Canine tissues were used for these experiments because the dog is a very common experimental animal and very little is known about the properties of its structural tissues. Furthermore dog's tissues are more easily available than human's.

Knowledge of the mechanical properties of the various tissues and organs in experimental animals is very important for artificial organs research since many prototypes are firstly used in animals (e.g. dogs, pigs, cows, sheep etc.) before they are used in humans.

#### A. Application to the Study of mechanical disfunctions

Previous workers studying mechanical disfunctions have concentrated mainly on arterial tissues. A number of studies have con-



sidered changes in the physical properties and histology of human arterial tissues with various diseases. These include observations of a rise in incremental Young's modulus with aging (27), possibly caused by an increase in the ratio of collagen to elastin fibres (28); a general deterioration in the quality of intra-arterial components in arteriosclerosis (28); and a study of the morphological factors that are important in the response of the aortic media to hypertension (45, 24). In addition, Burton (8) has suggested that arterial aneurysms are caused by a decrease in elastin fibre content without a corresponding increase in collagen fibres. This hypothesis is reasonable even though Sumner et. al. (42) failed to detect a change in the quantity of collagen and elastin in aneurysmal human arteries. It has also been observed that the absence of collagen from the aortic wall causes an increase in its extensibility (17). Although most of these studies have considered the aortic mechanical properties to be determined mainly by the collagenous and elastic networks of the vessel wall, the actual role of each tissue component in the deformation process is still a matter of considerable speculation (22, 29, 24). It is, however, precisely this information that is needed to establish a structural basis for the mechanics of normal tissues and determine, eventually, the histological origin of various tissue disfunctions.

#### B. Application to prosthesis

A second application of tissue mechanics lies in the use of aortic and other tissues in homograft or heterograft tissue replace-



ment (24). For instance, there is evidence that denaturation of implanted collagen may be a significant problem in aortic valve heterografts. Indeed, a number of authors have noted that the long-term success of these tissue implants is heavily dependent on the quality of their structural components (5, 9, 40). Hopefully a full understanding of tissue mechanics and its relation to the tissue components would help in the selection, preservation and implantation of tissue grafts (24). In addition, comparative studies of the mechanics and histology of animal and human tissues may help in assessing the relative merits of homografts and heterografts with respect to compatibility and long term function (24).

## 2. Prior Work

### Aortic tissue

Tissue mechanics of the cardiovascular system have been studied extensively from the year 1880 (41) to the present. Hass (18, 19) has attempted to correlate macroscopic mechanical properties to tissue structure. These investigations may be classified into one of two categories: mechanical and histological.

The mechanical studies are of two types: in vivo and in vitro. In vivo studies of static (35) and dynamic (36, 16) properties are relatively recent. The general results of the static properties work are that the aorta has an anisotropic elastic modulus which increases with intravascular pressure. The difficulties encountered with experiments on living animals make in vitro work more definitive (24).



The more common in vitro studies emanate from experiments on intact aortic segments (23), aortic rings (2, 3, 4, 19), or aortic strips (25, 26, 34). The intact segment work of which the most informative is that of Bergel (6), yields pressure-volume data that is nearly representative of the in vivo vessel. The aortic ring tests, best represented by Apter's extensive work (2-4), are amenable to many different types of testing procedures and can yield data about both the biomaterial making up the wall and the vessel itself. They lack in the estimation of properties that relate to two-dimensional stress such as isotropy. Finally, the aortic strip tests are the least representative of the intact aorta in vivo but provide the necessary data for estimating nearly all of the properties of engineering interest. Hence, they are the tests of choice in this work (24).

By far the most common representation of aortic mechanical data is in terms of arrangements of springs and dashpots (4, 34). These provide quantitative information about the tissue without representing its microstructure. There are also data presentation in terms of the theory of rubber elasticity (25, 26) and strain energy functions (13, 15). Both of these approaches may not be valid for tissues with two or more mechanically contributing components. The general conclusion of all these is that aortic tissue is a mechanically non-linear visco-elastic material for which some appropriately defined modulus increases with elongation (24).

#### Tendon

Abrahams (1) studied the mechanical behaviour of horse extensor tendon and human Achilles tendon in terms of the determination



of standard stress-strain curve (see Appendix 1), effects of cycling, effect of strain rate, determination of stress-relaxation and histological observations of both the strained and unstrained tendon. He also found that the stress-strain curve for successive cycles was reproducible provided that the strain on the specimen did not exceed 2.0-4.0%. If this strain level was exceeded, a permanent deformation occurred and this phenomenon was verified by histological studies on strained tendon which showed that some of the collagen fibres did not return to their original orientation (1). He also reported that the shape and position of the stress-strain curve were altered as the slope of the linear portion of the curve increased with increasing strain rate, although this is not as obvious from his data on figure 5 of (1).

Rigby et. al. (38) reported that increase in the rate of strain of rat tail tendons did not alter significantly the shape of the stress-strain curve. The main effect was an increase in the load required to produce a given strain. Experimenting with human extensor tendons Van Brocklin and Ellis (44) found that their elastic modulus progressively increased as the rate of stress application was increased. He also observed no change in mechanical behaviour as a result of preserving the tendon by freezing (44).

The physical characteristics of tendon include great tensile strength, flexibility, considerable inextensibility and almost perfect elasticity (11). There exists considerable variation in the estimates of the tensile strength of tendon (in the range of 5-10 kg/mm<sup>2</sup>) not only among different authors but within any one investigation, and



this may be attributed either to experimental error or to a real variation in the tensile strength relative to the collagen present. The latter could be due to variation of the cohesion between the collagen fibres, to variation of the molecular orientation within the tendon or, by analogy with the difference between stress-strain curves of nylon thread and nylon stockings, to some variation of the interweaving of the fibres (11). Partington and Wood (32) determined the role of non-collagen components in the mechanical behaviour of tendon fibres and they also found that the effects of enzymes on the mechanical properties of tendon suggests that an interfibrillar substance plays an important cohesive role in the stability of the collagen fibres (32). The influence of different interweaving patterns of fibres within tendons have not been investigated but the real difference of tensile strength in the collagen component of young and adult tendons may be due to a better orientation of the molecular chains in the adult (11). The effects of repetitive extension upon the physical properties of tendon collagen have been investigated by Rigby (39), who found, after an initial diminution, an increase of 35-40% in the "stiffness" of rat-tail tendon after about a thousand cycles each of less than 2% extension. He claims that if this cyclic extension is discontinued during an experiment the stiffness of the specimen continues to increase, and that complete recovery of the mechanical properties of a sample is only possible if it is rested in a slack condition for about 10 min. between extensions (39).



## Skin

Kenedi et. al. (21), experimenting with human skin, found that the load-deformation relations of human skin consist of a primary (low strain) and secondary (high strain) range, the former appearing to be age dependent. When load is applied to skin, the initial deformation mechanism, both in vitro and in vivo appears to be one of straightening and load orientation of the collagen bundles, culminating at higher load levels in a fully orientated and virtually closely packed structure. At the biological stress levels encountered in clinical practice it appears that this network deformation is the controlling factor in the overall load-deformation relation of skin, rather than the mechanical characteristics of the collagen itself (21). A feature of particular clinical significance of this overall load response of skin is the contraction shown (both in vitro and in vivo) at right angles to the applied tension. This contraction is load dependent, is fully comparable to the extension obtained in the direction of the applied tension and influences materially the design of reparative procedures in plastic surgery (21).

Finlay (12) made an in vivo study of human skin. He designed and built a device which was used to investigate fully the non-linear viscoelastic properties of skin by applying a torsional load to the skin in vivo. This resulted in the residual alignment of dermal fibres due to the action of the torsional strain — the fibre rearrangement being dependent on the magnitude of the strain applied (12).

Ridge and Wright (37) verified the phenomenon of Langer's



Lines and showed that they are lines of principle tension in the skin. Histological work showed that the lines also follow the direction of general orientation of the fibres (37).

Gibson et. al. (14) found a directional variation in the extensibility of human skin on uniaxial loading in the plane of the skin. This report (14) dealt with a pilot study of this characteristic as observed on the anterior aspect of the chest and they concluded that there is a correlation between this anisotropy in extensibility and Langer's Lines. They also found the direction of maximum extensibility to be at right angles to the Langer's Lines which further substantiated the hypothesis that Langer's Lines represent a preferred orientation of the fibres within the dermis (14).

A mechanochemical method was developed by Yannas and Huang (47(a)) for studying the enzymatic degradation of insoluble collagen fibres. The method involves stretching the collagen fibre to a fixed extension in the presence of a solution of collagenase and measuring the rate of relaxation of the force induced on the fibre. Yannas and Huang (47(a)) observed an exponential decrease in force with time. The slope of the linear plot of logarithm of the force vs. time was taken as a measure of the rate of enzymatic degradation. This rate was found to vary with collagenase concentration, pH, temperature, and changes in cross link density of collagen fibre (47(a)). This method is found useful in the design of collagenous implants with specified resistance to enzymatic degradation in vivo. It also provides a simple method for screening in vitro a variety of modified collagens for use as connective tissue replacement in surgery (47(a)), 47(b)).



### Cornea and Sclera

To the author's best knowledge the only related work done on the dog's cornea and sclera are those by Yamada (46) where he determined their tensile (stress-strain curve) and expansive (pressure-volume curve) properties.

### Histologic Work

The gross histology of the tissues studied are sufficiently known to be found in standard histology texts (7). Abrahams (1), in his work on the mechanical behaviour of horse and human tendon, supported his observations by histological micrographs of strained and unstrained tendon using haematoxylin and eosin (H&E) staining technique. He managed to show the eventual straightening of the collagen fibres of the strained tendon. Lake (24) carried out similar histological studies on the human and bovine aortic tissues using Verhoeff's and Aniline blue stains. Missirlis (30) did more extensive histology on the human aortic valve to show the structural organization of elastin, collagen and lipids. He utilized a more varied staining technique including Verhoeff's, Aniline blue, Aldehyde-Fuchsin, Trichrome and others (30).

### 3. Structure of the Various Tissues

The following paragraphs, which discuss the structure of the various tissues, are taken from the standard histology text by Bloom and Fawcett (7).

#### Aorta

Generally, the aorta consists of three layers which are: the tunica *intima*, internally and bordering the lumen; the tunica media;



and the tunica adventitia, externally.

The tunica intima, although the thinnest of the three (45-68  $\mu$ ) is often subdivided. The intima of the aorta consists of the endothelium, a layer of subendothelium connective tissue, with fibroblasts and with fibres chiefly of the collagenous type, and the internal elastic membrane. The tunica media is a relatively thick layer and contains abundant elastic tissue. Here, the second important tissue of the media, the smooth muscle, is relatively inconspicuous (7).

Outside the media is a layer of connective tissue, the adventitia. This layer contains the important vasa vasorum, those vessels carrying blood for the supply of the tissue of the wall of this large artery (7).

The differing characteristics of these three layers are such that the intima and media elastic structures distend greatly as the blood is forced into the artery but the adventitia, less elastic but with a high tensile strength, helps to restrain the expansion of the first two layers (7).

The smooth muscle of the media appears to be arranged chiefly in a circular manner, the fibres running parallel to the circumference of the vessel (7). There is evidence, however, that in four arteries at least, the actual direction is a spiral one. The muscle alternates with lamellae of elastic fibres. Studies have shown that the fibres of smooth muscle can accumulate lipid deposits; their part in the development of arteriosclerosis may be more important than has been thought (7).

### Skin

The skin consists of two layers: the outer epidermis, an almost wholly epithelial layer, and the inner dermis, a connective tissue



layer. Beneath the skin lies the superficial fascia, sometimes called the hypodermis. This fascia has abundant adipose tissue in it in various regions of the body, as in the abdominal area. It lies over the deep fascia covering the surfaces of the skeletal muscles.

The functions of the skin are several: protection of the underlying tissue; reception of external stimuli; and regulation of body temperature (7).

The epidermis is a stratified squamous epithelium, varying in number of layers of cells, and hence in thickness, in different regions of the body. Its outermost layer is always keratinized or cornified, formed by sheets of dead cells (7).

The dermis is a connective tissue layer. Its blood vessels have the function of nourishing not only its own tissue but also the epidermis. The bulk of the dermis is collagenous with a widespread network of elastic fibres (7). This accounts for the highly extensible characteristic of skin. These fibres are concentrated about the cutaneous glands and hair follicles and form a fine network beneath the epidermis (7).

#### Tendon

The primary function of tendon is to transmit force and its structure is admirably suited to this function. The most striking feature of the collagenous mesh is the bundling of fibres into almost parallel arrays to define the principal axis of the tendon itself (7). The bundles are retained loosely by connective tissue (the paratenon) which includes elastic fibres (7). Where lubrication is necessary, the tendon is constrained within a sheath of small or large extent, catering for



one or several tendons. The tendon is contained within a delicate covering layer, the epitenon, which appears silky in texture and which exhibits a transverse pattern which is identified with a physical periodicity of the underlying microstructure (7). The primary parallel running fibrils of collagen form (by plaiting) secondary bundles, the fasciculi, which intermesh to produce helicoidal bundles of fibres (7). Tendon is deficient in elastic fibre (7); Elliott (11) gives, for the tendon calcaneus of man, a figure of 2% of dry weight, or 0.8% of wet weight. The highly orientated arrangement of collagen bundles and the low elastin content account for the high tensile strength and Young's modulus, and low elastic limit of tendon, commensurating with its function as a force transmitting device.

#### Sclera

The sclera forms the posterior four-fifths of the eyeball and is continuous anteriorly with the cornea. It has a thickness of about 0.5 mm. The sclera consists of dense fibrous tissue arranged in a rather irregular fashion, unlike that in the cornea (7) (see Histology section of this report); there is also much more elastic tissue than in the cornea (7) (not shown by our histology). The tendons of the extrinsic eye muscles are continued into the sclera in order to provide rotation of the eyeball (7). The facile motion of the eyeball may be better understood when one sees at the outer surface of the sclera how loose the arrangement of the collagenous bundles is (7). The cleft spaces here are called Tenon's spaces.

#### Cornea

This is the transparent anterior continuation of the sclera,



and consists of five well-defined layers: external stratified epithelium, Bowman's membrane, stroma or substantia propria constituting the main mass of the cornea, Descemet's membrane, and an inner layer of squamous epithelium (7).

The stroma or substantia propria is continuous with the sclera and consists of very regularly arranged lamellae of collagen fibres (7) (see Histology). In each layer the collagen fibres are parallel with one another, but in adjacent layers the fibres change direction and are roughly at right angles to the fibres in the next layer (7). The layers also exchange fibres and the whole is held together by a mucoprotein which is highly sulphated and rich in keratan sulphate. As the fibres and mucoprotein have the same refractive index and are highly hydrated, the whole cornea is transparent (7). Between the lamellae are very irregularly shaped flattened cells called keratocytes (7). The transparency of the cornea admirably suits its function as a structure through which light rays from external objects have to penetrate before being focussed by the lens on to the retina.

#### 4. Composition

All the tissues examined contain elastin, collagen, lipids and mucopolysaccharides. The aorta contains an extra component viz. smooth muscle (24). The proportions of the various components vary from one tissue to another, e.g. aortic tissue and abdominal skin contain a relatively high percentage of elastin (24, 14) than cornea, sclera and tendon (all of the last three of which are essentially collagenous). Elliott (11) quoted a figure of 70% (dry weight) for the collagen content of dog's tendon.



The mechanical contribution of collagen, elastin and lipids has been determined by Lake (24) for human and bovine aorta. Hoffman et. al. (20) have shown the mucopolysaccharides to be unimportant in the stress bearing function of aortic tissue. This study will determine the contribution of elastin, collagen and mucopolysaccharides to the stress-strain characteristics of the various tissues and to correlate these with the histological studies of the respective tissues.



## MECHANICS OF TISSUES

### 1. Experimental Procedure

Throughout this work the word sample will refer to the tissue strips used for mechanical tests. These strips are taken from the circumferential and longitudinal directions of the tissue wherever possible e.g. as in the case of the aorta (see Figure 1).

All tissues for mechanical tests are taken from dogs, within the age range 5-8 years old, sacrificed in the Cardiorespiratory Unit of McMaster University Medical Centre. These tissues were removed shortly after death (within 2-3 hours) and refrigerated at 3°C in 0.9% saline solution with small amounts of penicillin and gentocin added in to check biological degradation. In all cases the samples were used within a period of 3-5 days.

The methods of component extraction were selected to completely remove a particular component while minimizing degradation to the remaining material. Collagen was removed by steam autoclaving under water at 15 p.s.i.g. (120°C) for about six hours. This procedure was chosen over a number of others (33) as the least degradative on the remaining tissue. Selective removal of elastin was accomplished by means of an enzymolytic treatment using a 50-50 mixture of elastase and trypsin inhibitor (300 µg per ml. buffer at a pH of 8.6) for 5 hours at 22-25°C in a shaker bath. This treatment removes most of the elastin without causing any measurable degradation in the mechanical properties



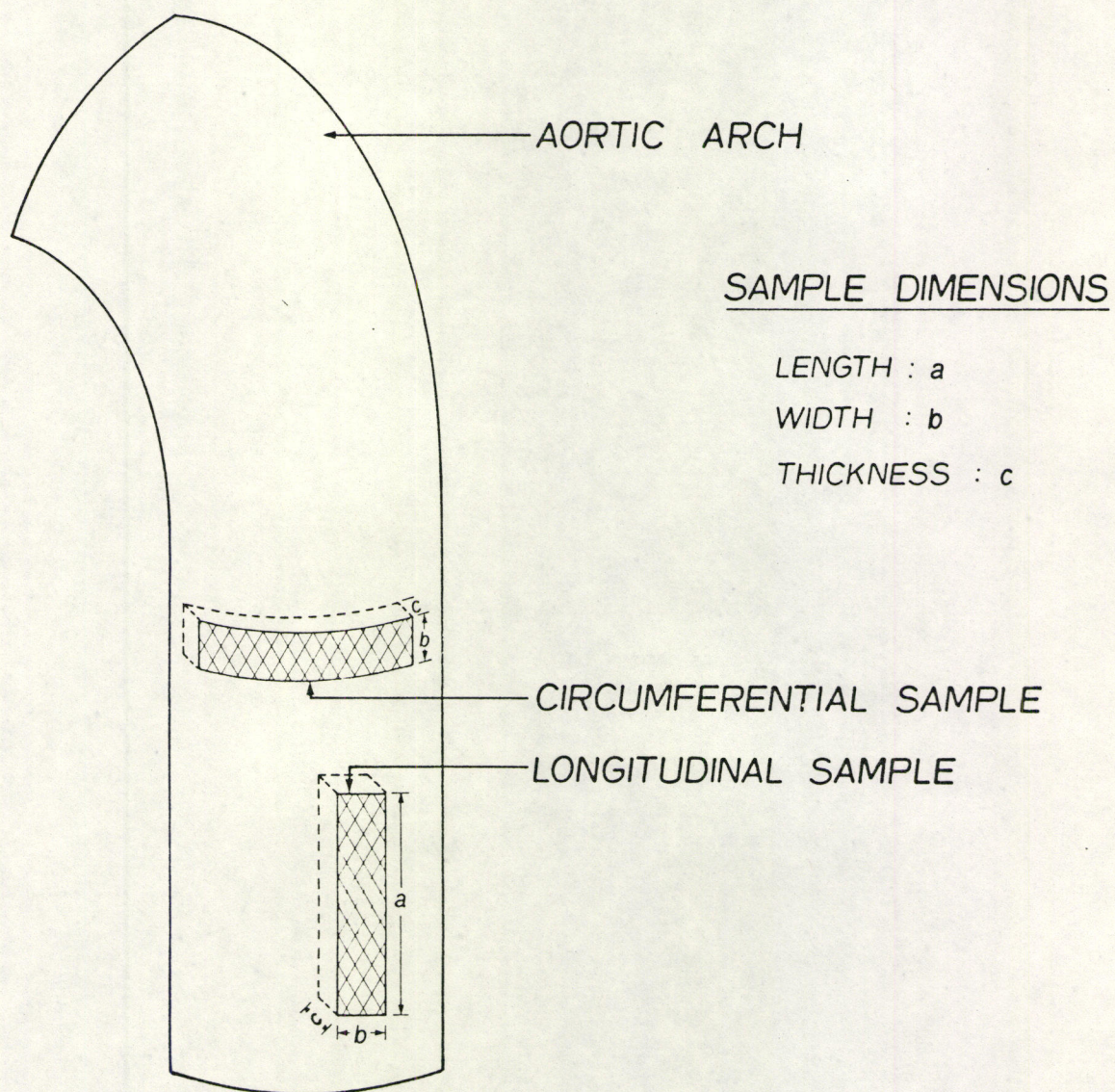


Fig. 1: Orientations of samples in descending aorta (similarly in ascending aorta)



of the collagen in the tissue (30). The mucopolysaccharides were removed by treating the tissues with hyaluronidase (from bovine testes) in the ratio of enzyme: substrate = 1:20 in a buffer of 0.01 M sodium acetate adjusted to a pH of 4.8 for 100 hrs at 37°C (20).

The samples used for mechanical testing were cut with a scalpel into rectangular strips about 3-5 mm wide. The strip lengths were at least 10 mm long for the sample to be free of end effects in the mechanical tests.

All measurements of the stress-strain characteristics were performed on a "Universal Tensile Testing Instrument" (Model U.T.M.-II-20 with a maximum load capacity of 20 kg, manufactured by Toyo Baldwin Co. Ltd.) with the sample immersed in saline solution at room temperature. Two important parameters, needed to determine stress and strain, are the cross-sectional area,  $A$ , of the sample and its initial length  $l_0$ . The initial cross-sectional area,  $A_0$ , was measured optically, with the immersed sample in position between the two tensile machine grips, at zero load. A mirror, placed at 45° angle gave a projection of the sample edge at the same plane as its side. Thus the width and thickness of the sample were measured through the microscope by means of a calibrated eyepiece. The initial length of the sample was also determined optically with the stereomicroscope at the moment of initial deflection of the load recorder pen on the machine.

Two types of load cells were used according to the type of tissue, and in all considered cases there was neither clamp slippage nor breakage of the sample. The stress-strain curves were always obtained from the loading cycle and were used to calculate engineering stress and



tangential modulus (see Appendix 1).

In all the tensile stress-strain experiments a hysteresis loop was observed, and its area stabilized after the second test on the same sample. Also in all the cases the first test gave a different curve from the subsequent ones and was disregarded. This phenomenon has been previously observed by Rigby *et. al.* (38) and he termed it a "conditioning stretch", which produces a slight permanent elongation and is never recovered.

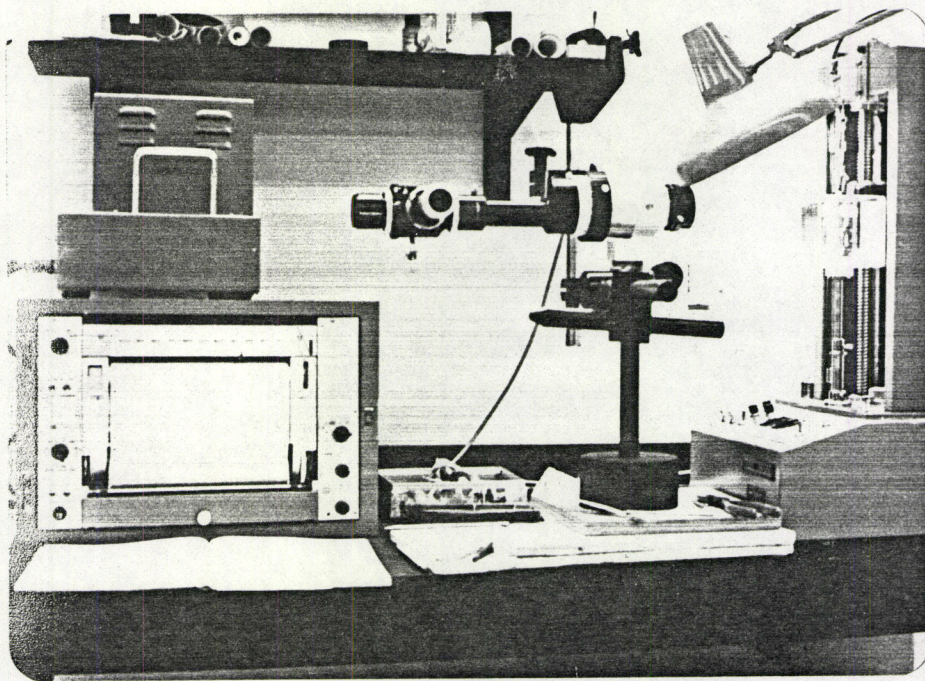
All the tensile data were taken at a constant cross-head speed of 2 mm/min.

Figure 2 shows the experimental set up with a close-up on the sample.

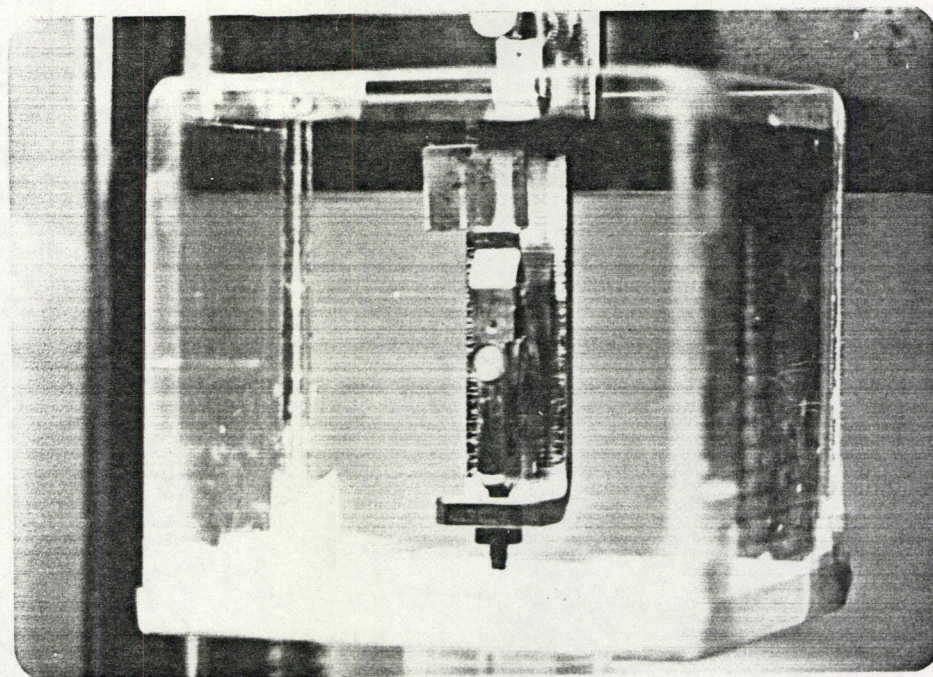
## 2. Results

Figures 3 and 4 show typical stress-strain curves of the dog's descending aorta in the circumferential and longitudinal directions respectively in the native state, after deelastination and after decolagenation. Table 1 indicates the high and low strain moduli in the circumferential and longitudinal directions.





(a)



(b)

Figure 2: (a) Experimental set up  
(b) Close-up on sample



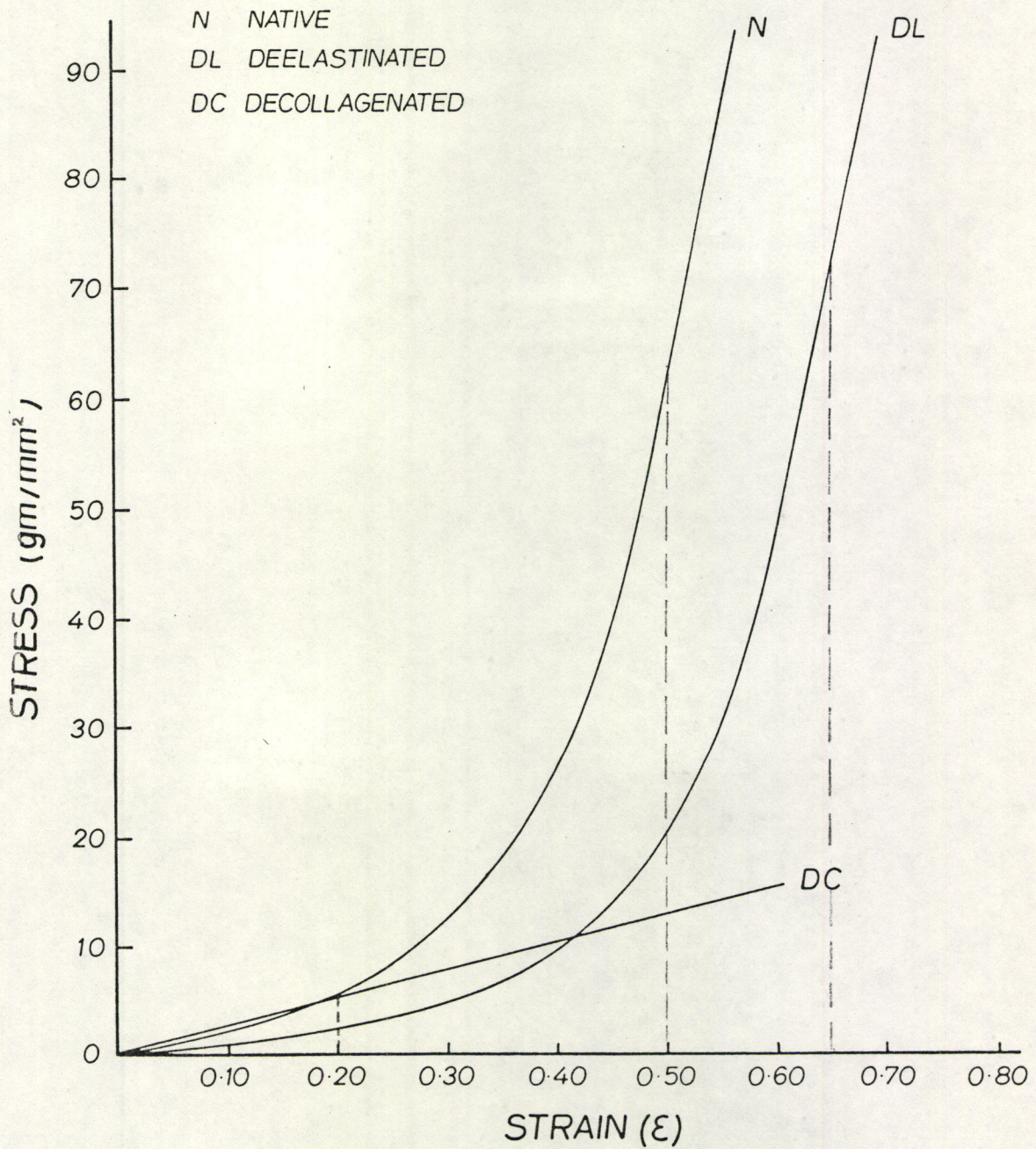


Fig. 3: Typical stress-strain curves of dog's descending aorta (circumferential sample).



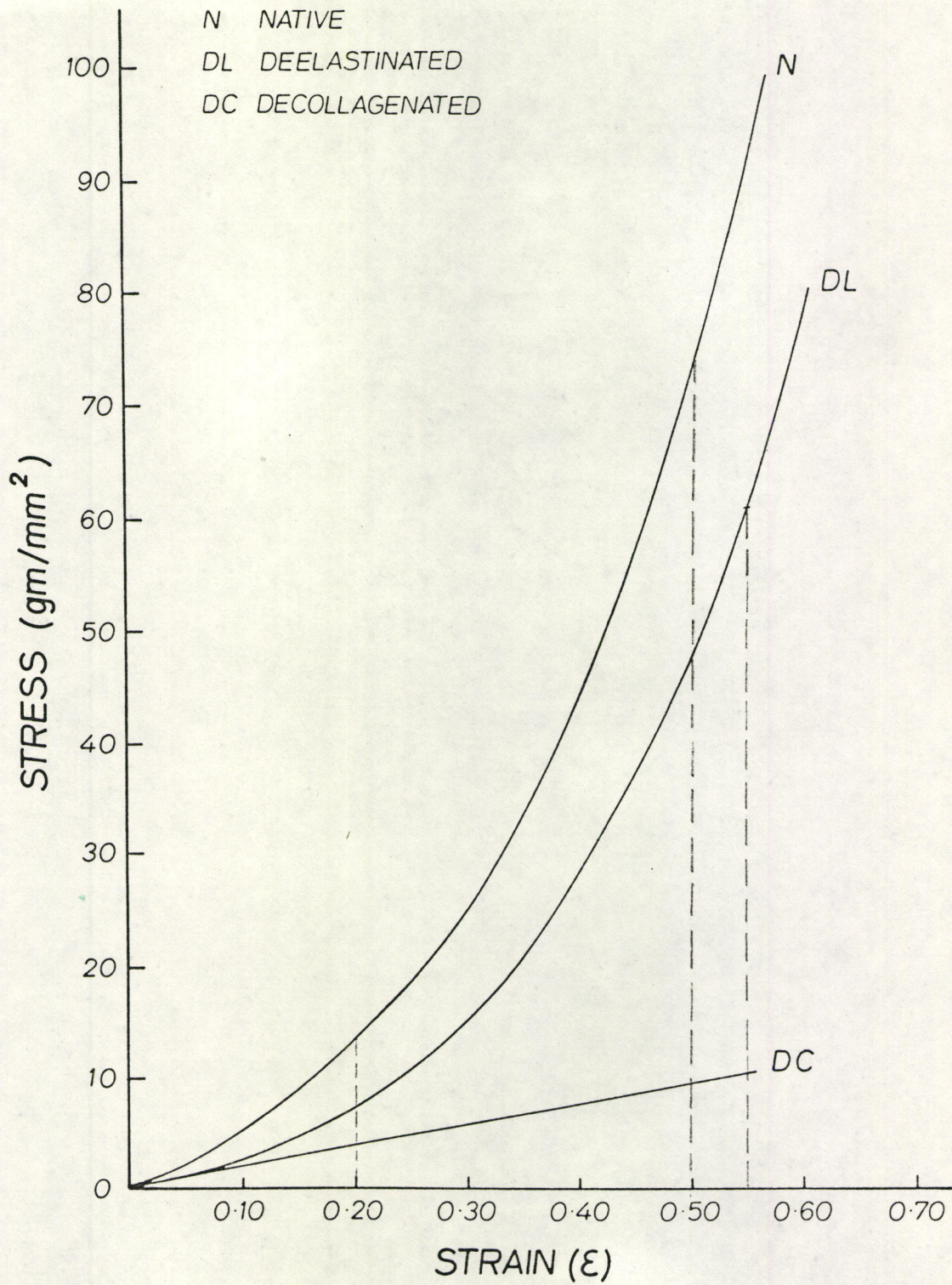


Fig. 4: Typical stress-strain curves of dog's descending aorta (longitudinal sample)



Descending AortaLow Strain Moduli ( $\epsilon = 0.2^*$ )

<u>Number of Samples</u>	<u>Direction of Stress</u>	<u>Eavg (gm/mm<sup>2</sup>)</u>	
		<u>Native</u>	<u>Deelastinated</u>
5	Circumferential	12.33 (2.15)†	10.22 (3.91)
5	Longitudinal	18.55 (4.20)	10.76 (3.84)

High Strain Moduli

5	Circumferential	737.8 ( $\epsilon=0.5^*$ ) (67.39)	790.22 ( $\epsilon=0.65$ ) (46.58)
5	Longitudinal	353.9 ( $\epsilon=0.5$ ) (63.57)	327.7 ( $\epsilon=0.55$ ) (54.86)

\*  $\epsilon$  = value of strain at which modulus is calculated.

† Figures in parantheses denote standard deviation in groups.

TABLE 1: Variation in Modulus of Native and Deelastinated Dog's Descending Aorta



Figs. 5 and 6 show typical stress-strain curves for the ascending aorta in the native, deelasinated and decollagenated state in the circumferential and longitudinal section respectively. Table 2 indicates the high and low strain moduli for the native and deelasinated tissue.

Figs. 7 and 8 show typical stress-strain curves for the dog's abdominal skin in the longitudinal (parallel to the long axis of the body) and in the transverse or circumferential (perpendicular to the long axis) section. Table 3 shows the variation in modulus of the native and deelasinated skin.

Fig. 9 shows typical stress-strain curves for the dog's Achilles tendon while Table 4 indicates the variation in modulus of the native and deelasinated tendon.

Figs. 10 and 12 show typical stress-strain curves for the cornea and sclera respectively while Tables 5 and 6 show the variation in moduli of the native and deelasinated tissues.

Figs. 13, 14, 15 show the stress-strain curves for the native and mucopolysaccharides (MPS)-free samples from the ascending aorta, the Achilles tendon and the cornea of the dog. There is virtually no difference between the native and the MPS-free tissues which confirms Hoffman's (20) observations.



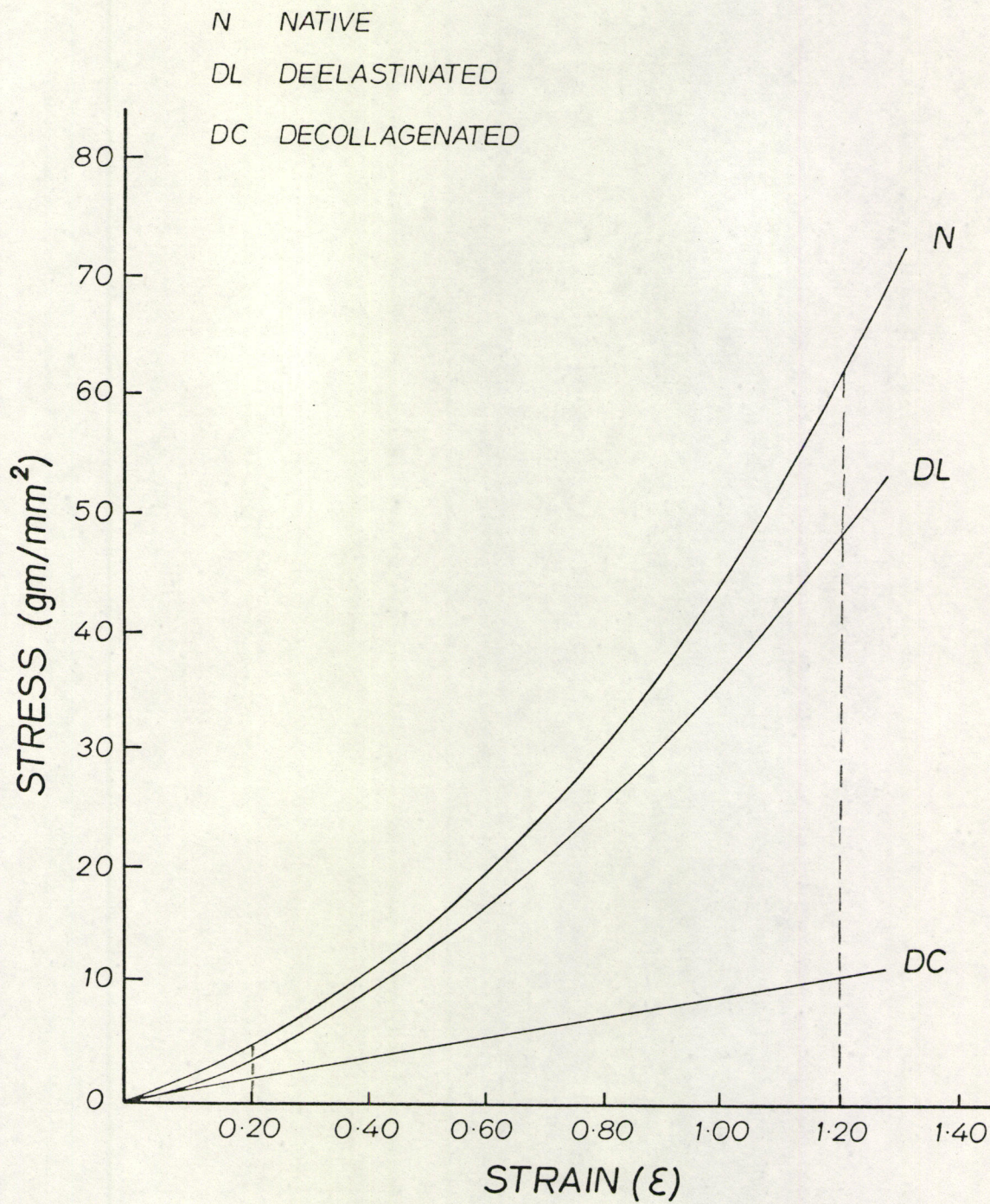


Fig. 5: Typical stress-strain curves of dog's ascending aorta (circumferential sample)



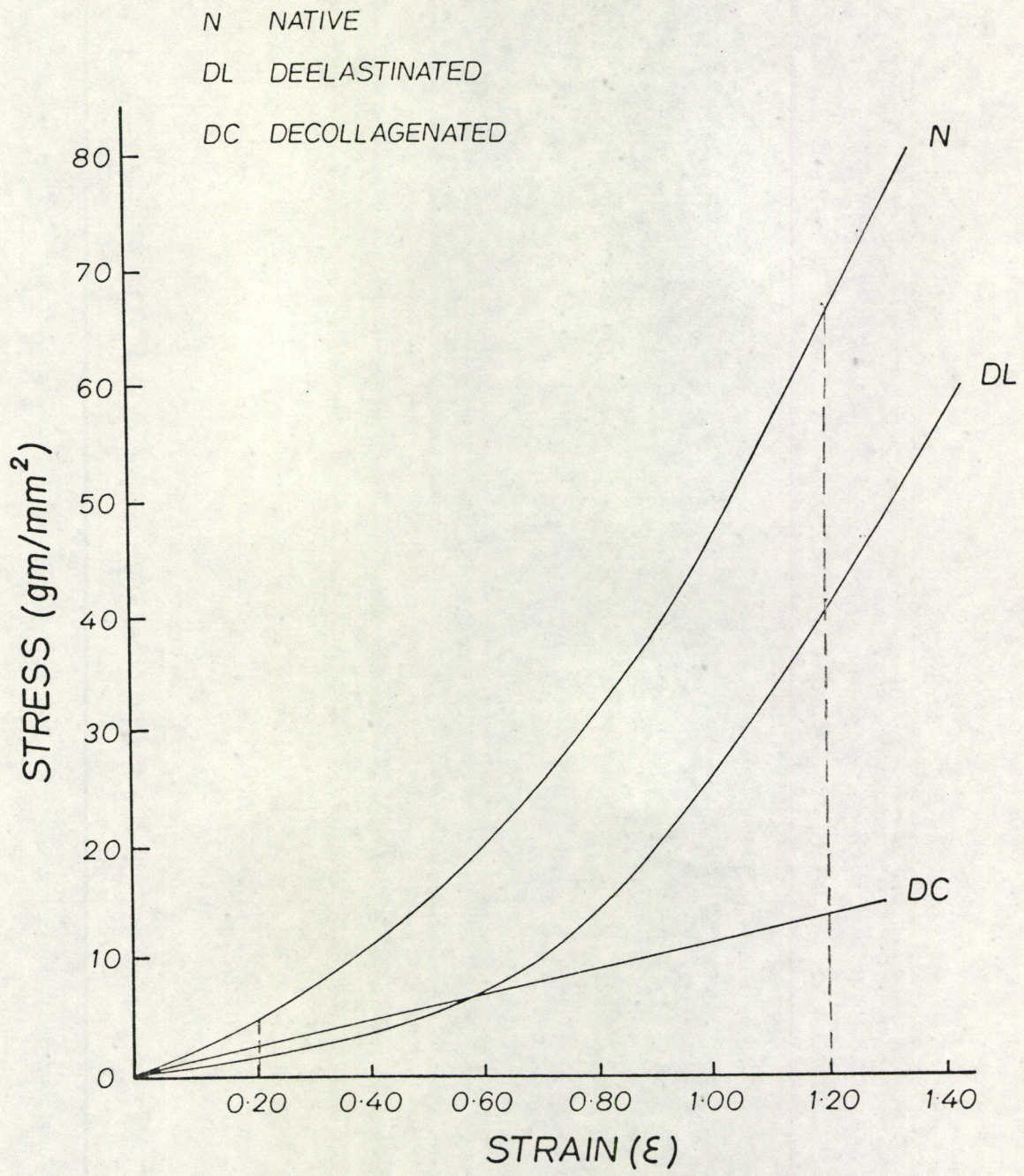


Fig. 6: Typical stress-strain curves of dog's ascending aorta (longitudinal sample)



ASCENDING AORTALow Strain Moduli ( $\epsilon = 0.2$ )Eavg (gm/mm<sup>2</sup>)

<u>Number of Samples</u>	<u>Direction of Stress</u>	<u>Native</u>	<u>Deelastinated</u>
10	Circumferential	27.22 (3.20)	21.49 (2.73)
10	Longitudinal	28.59 (3.78)	5.06 (1.54)

High Strain Moduli ( $\epsilon = 1.20$ )

10	Circumferential	98.68 (15.01)	64.31 (14.65)
10	Longitudinal	100.19 (13.77)	75.50 (13.77)

TABLE 2: Variation in Modulus of Native and Deelastinated Ascending Aorta



N NATIVE  
DL DEELASTINATED  
DC DECOLLAGENATED

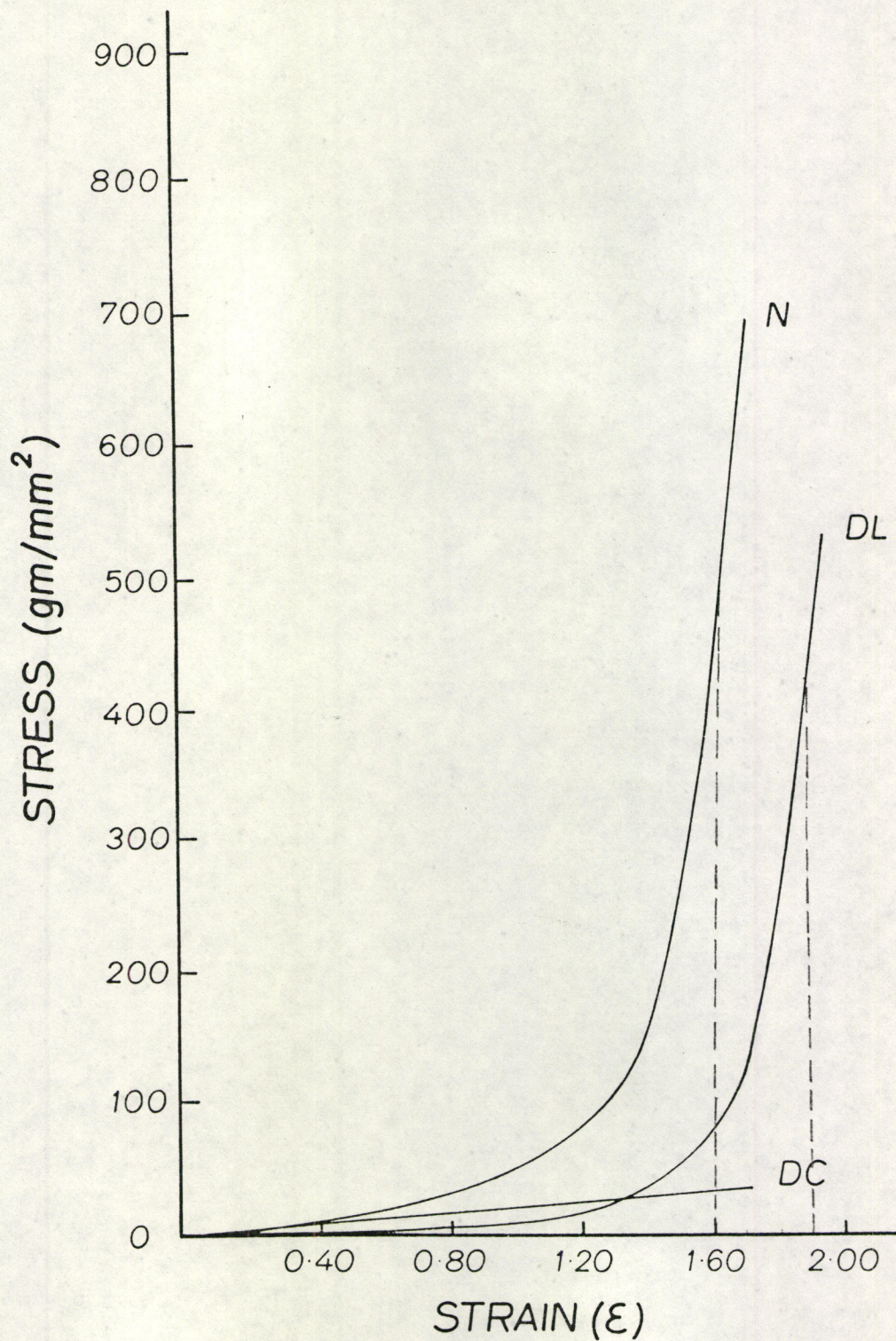


Fig. 7: Typical stress-strain curves of dog's abdominal skin (longitudinal sample)



N NATIVE  
DL DEELASTINATED  
DC DECOLLAGENATED

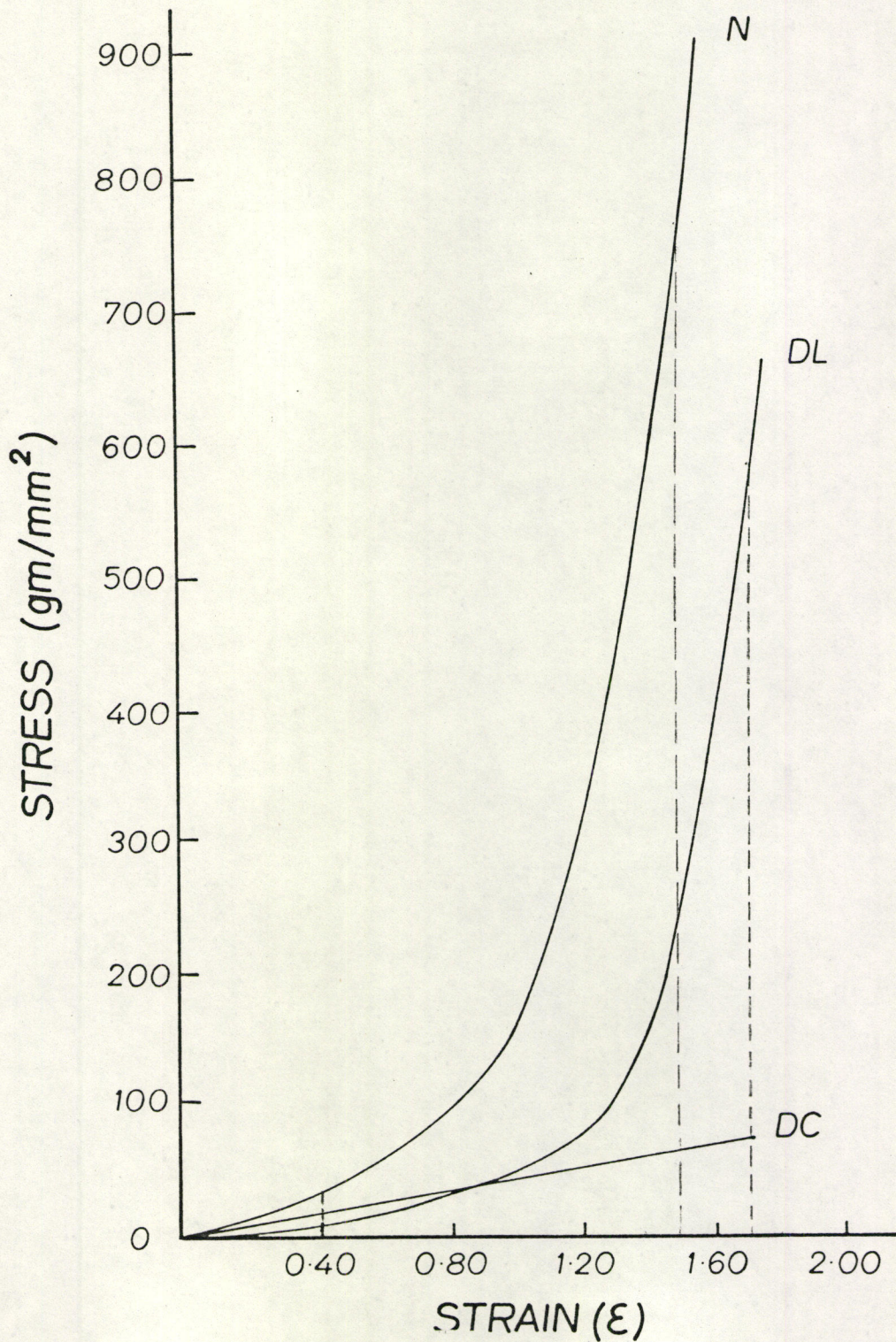


Fig. 8: Typical stress-strain curves of dog's abdominal skin (transverse sample)



ABDOMINAL SKINLow Strain Moduli ( $\epsilon = 0.40$ )

Number of Samples	<u>Direction of Stress</u>	<u>Native</u>	<u>Deelastinated</u>
5	Transverse	87.50 (7.27)	43.48 (3.53)
5	Longitudinal	25.00 (3.25)	12.50 (1.57)

High Strain Moduli

5	Transverse	1908.9 ( $\epsilon=1.50$ ) (52.45)	1602.3 ( $\epsilon = 1.70$ ) (22.15)
5	Longitudinal	1875 ( $\epsilon=1.6$ ) (27.91)	2164.8 ( $\epsilon=1.9$ ) (66.70)

TABLE 3: Variation in Modulus of Native and Deelastinated Abdominal Skin



N NATIVE  
DL DEELASTINATED  
DC DECOLLAGENATED

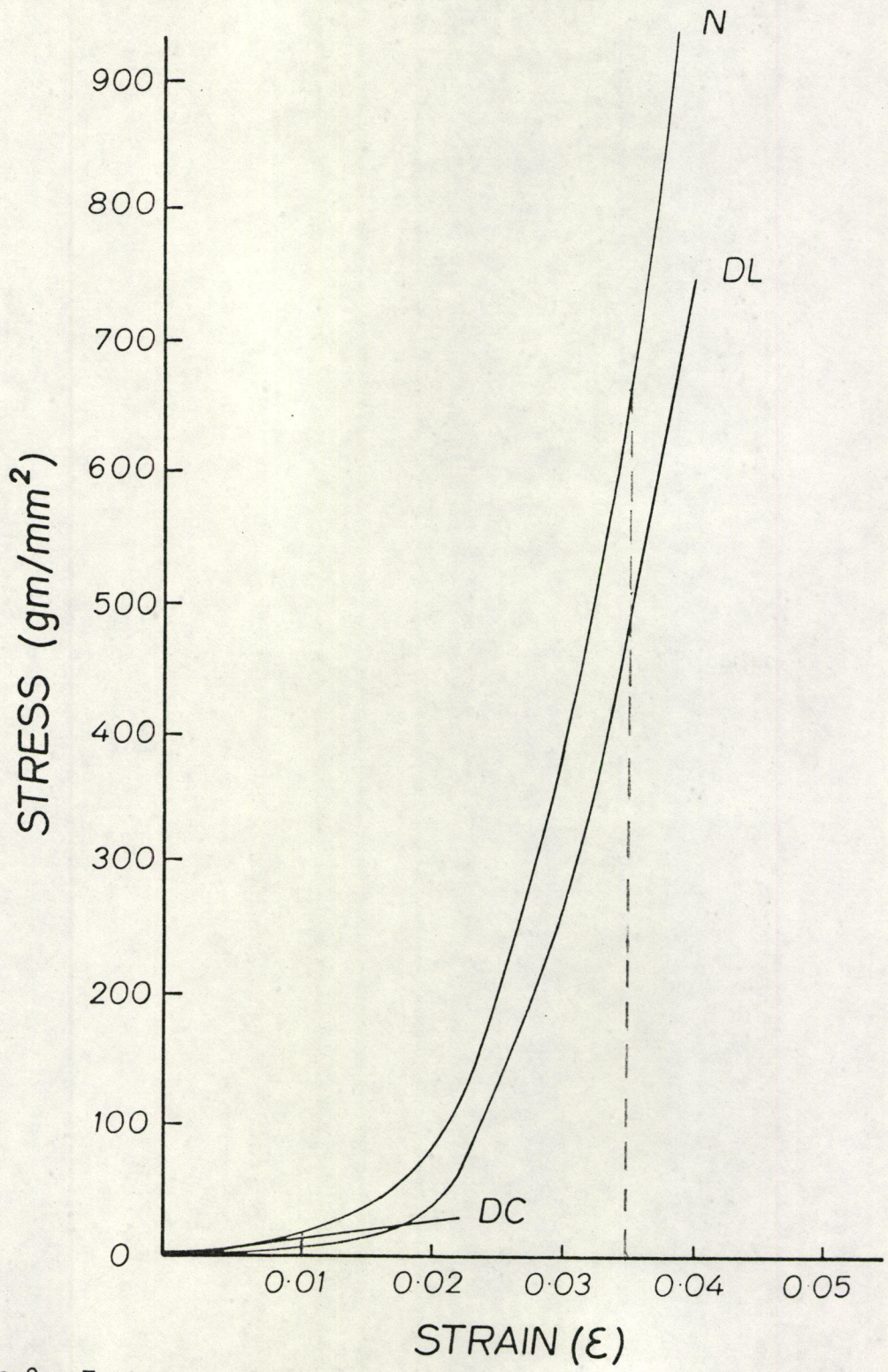


Figure 9: Typical stress-strain curves of dog's Achilles tendon



ACHILLES TENDONLow Strain Moduli ( $\epsilon = 0.01$ )

<u>Number of Samples</u>	<u>Direction of Stress</u>	<u>Eavg (gm/mm<sup>2</sup>)</u>	
		<u>Native</u>	<u>Deelastinated</u>
10	Longitudinal	1995.2 (83.79)	651.54 (10.74)

High Strain Moduli ( $\epsilon = .035$ )

10	Longitudinal	59368.0 (2147.3)	57815.0 (1569.0)
----	--------------	---------------------	---------------------

TABLE 4: Variation in Modulus of Native and Deelastinated Achilles Tendon



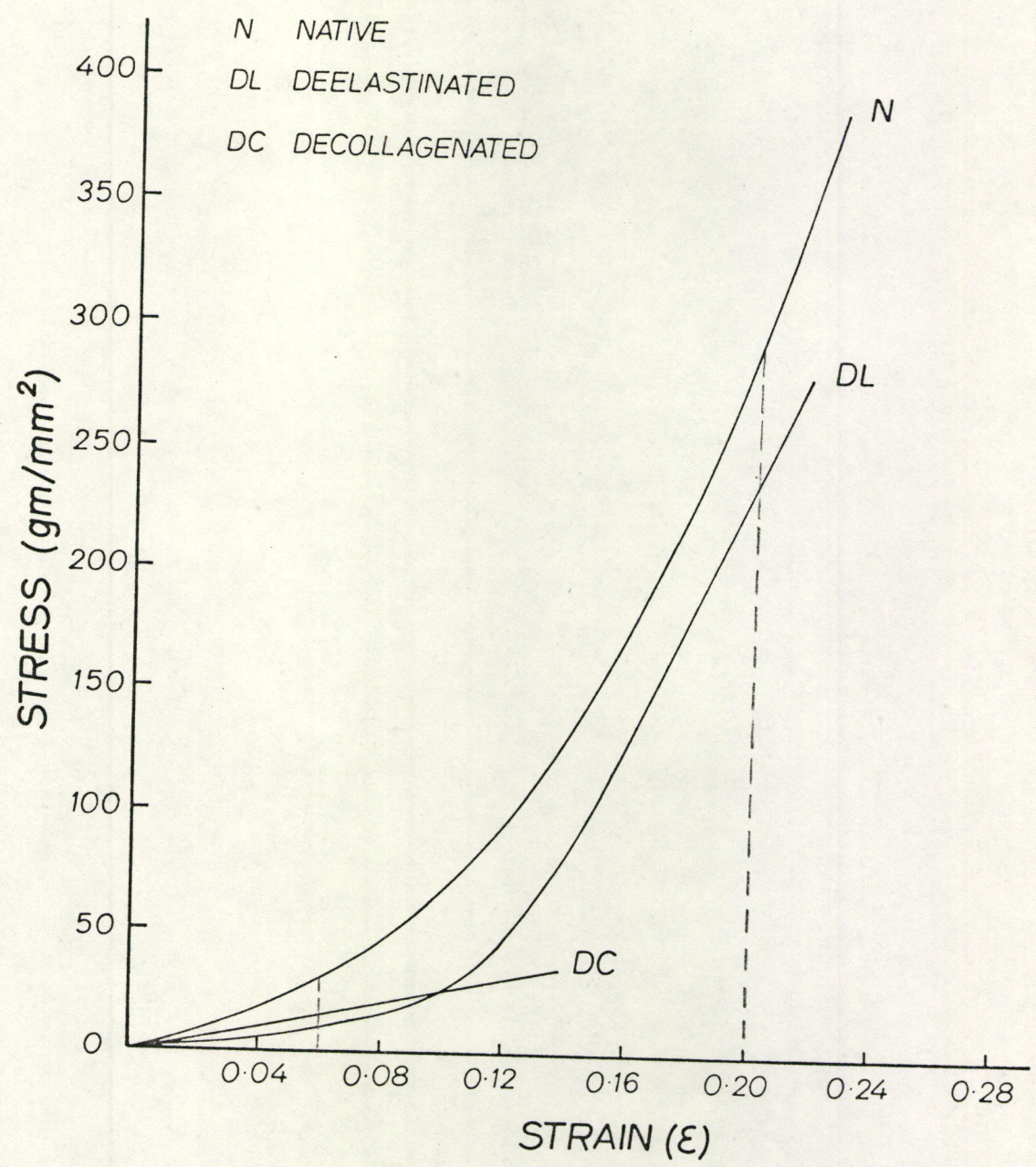


Figure 10: Typical stress-strain curves of dog's cornea



CORNEALow Strain Moduli ( $\epsilon = 0.06$ )Eavg. ( $\text{gm/mm}^2$ )

<u>Number of Samples</u>	<u>Direction of Stress</u>	<u>Native</u>	<u>Deelastinated</u>
10	Meridional*	623.44 (17.84)	233.40 (14.91)

High Strain Moduli ( $\epsilon = 0.20$ )

10	Meridional	2953.40 (164.71)	2537.50 (31.98)
----	------------	---------------------	--------------------

\* See Fig. 11 for explanation of "Meridional"

TABLE 5: Variation in Modulus of Native and Deelastinated Cornea



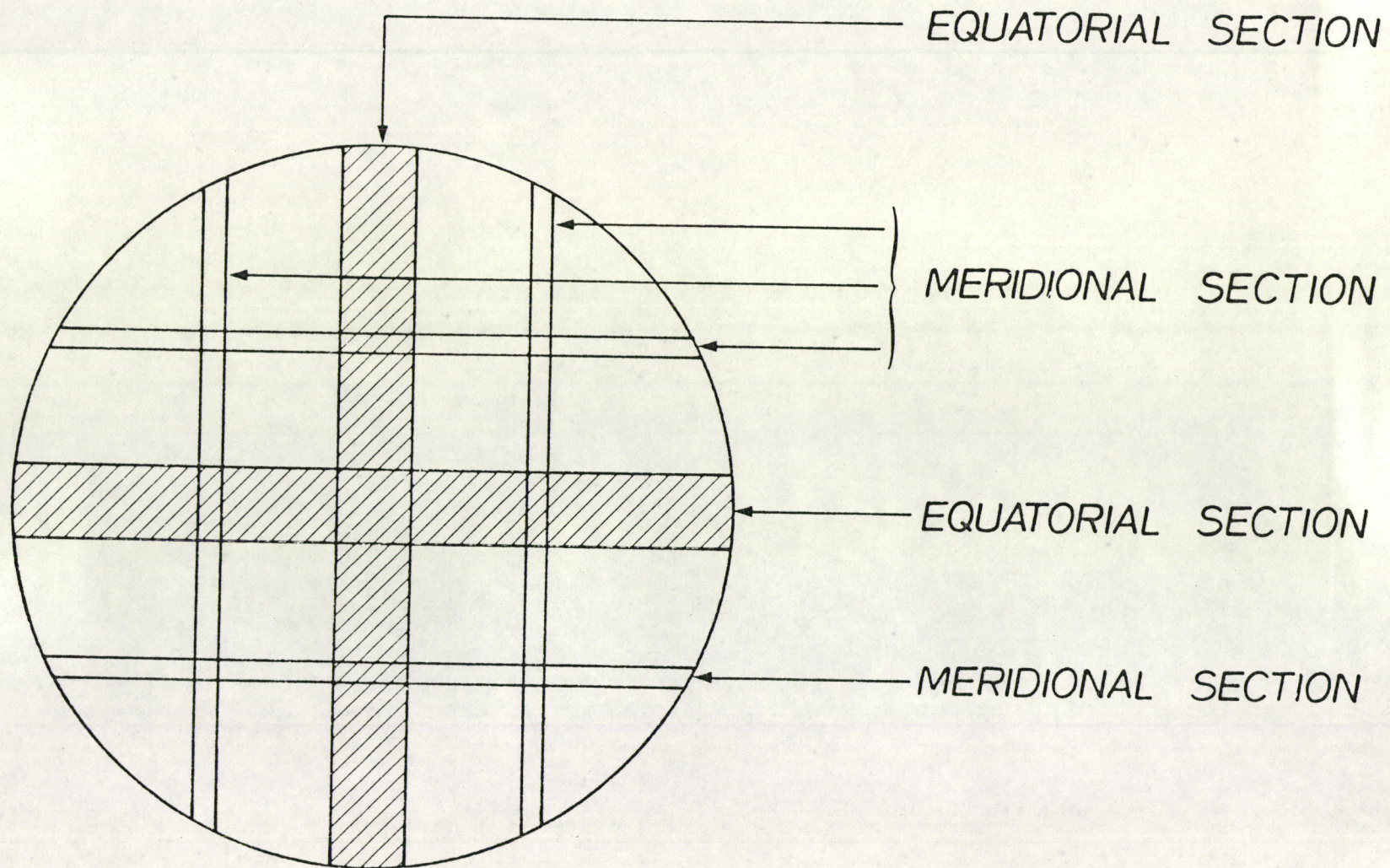


Figure 11: Schematic diagram of cornea showing equatorial and meridional sections



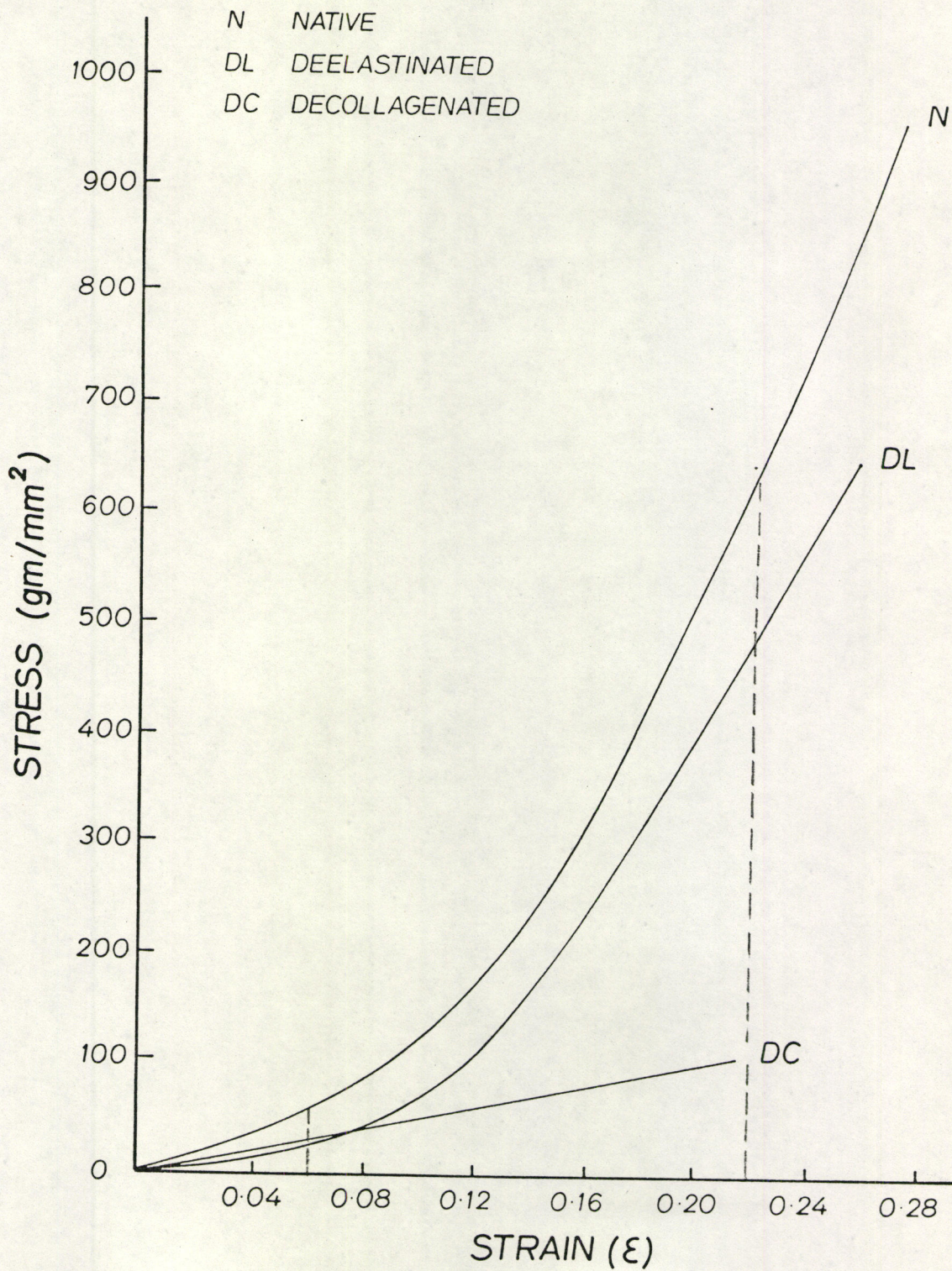


Figure 12: Typical stress-strain curves of dog's sclera



SCLERALow Strain Moduli ( $\epsilon = 0.06$ )

<u>Number of Samples</u>	<u>Direction of Stress</u>	<u>Eavg (gm/mm<sup>2</sup>)</u>	
		<u>Native</u>	<u>Deelastinated</u>
10	Meridional	1251.70 (10.46)	689.0 (9.06)

High Strain Moduli ( $\epsilon = 0.22$ )

10	Meridional	5445.20 (139.70)	4479.60 (89.40)
----	------------	---------------------	--------------------

TABLE 6: Variation in Modulus of Native and Deelastinated Sclera



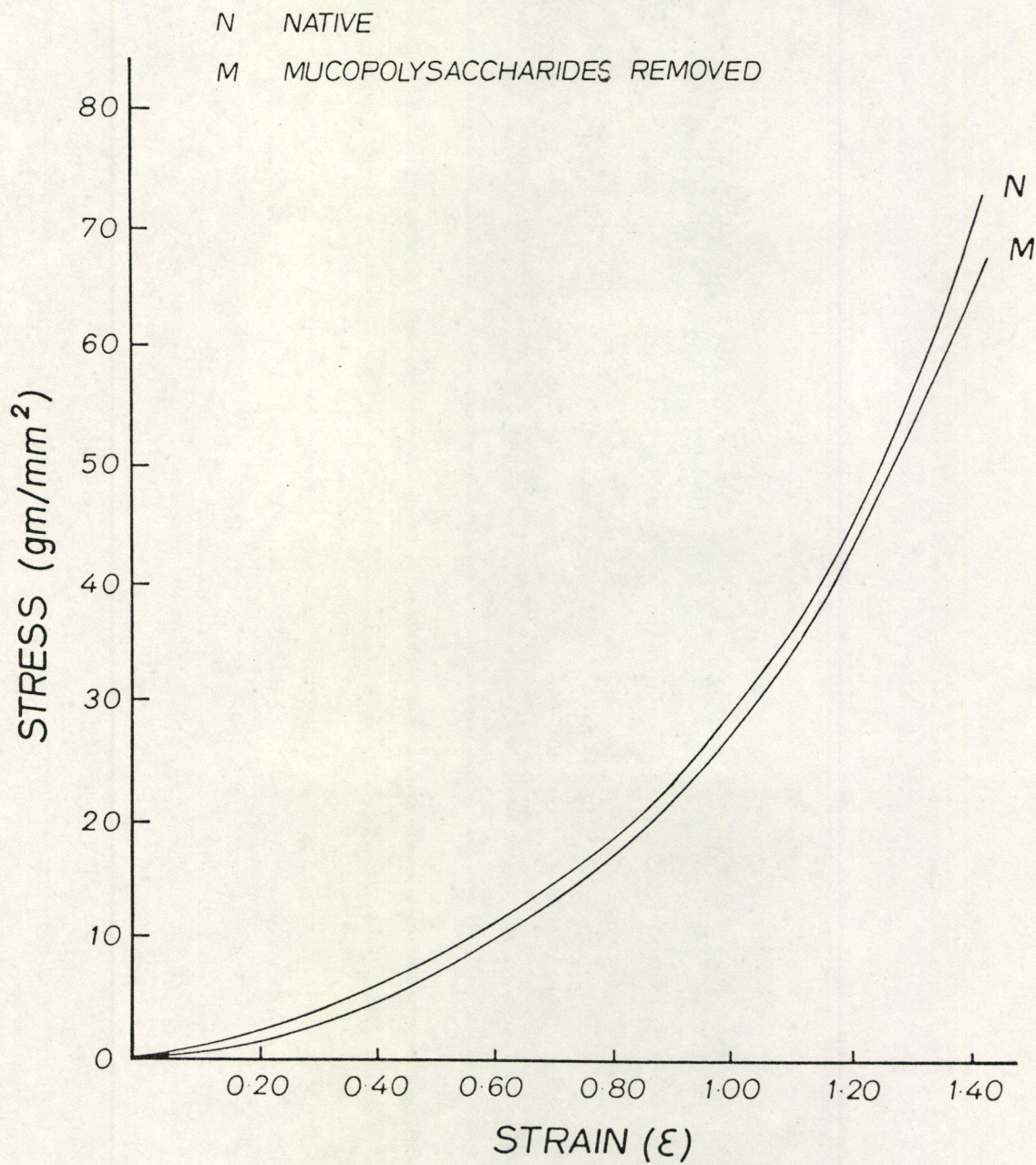


Figure 13: Typical stress-strain curves of dog's ascending aorta (circumferential sample)



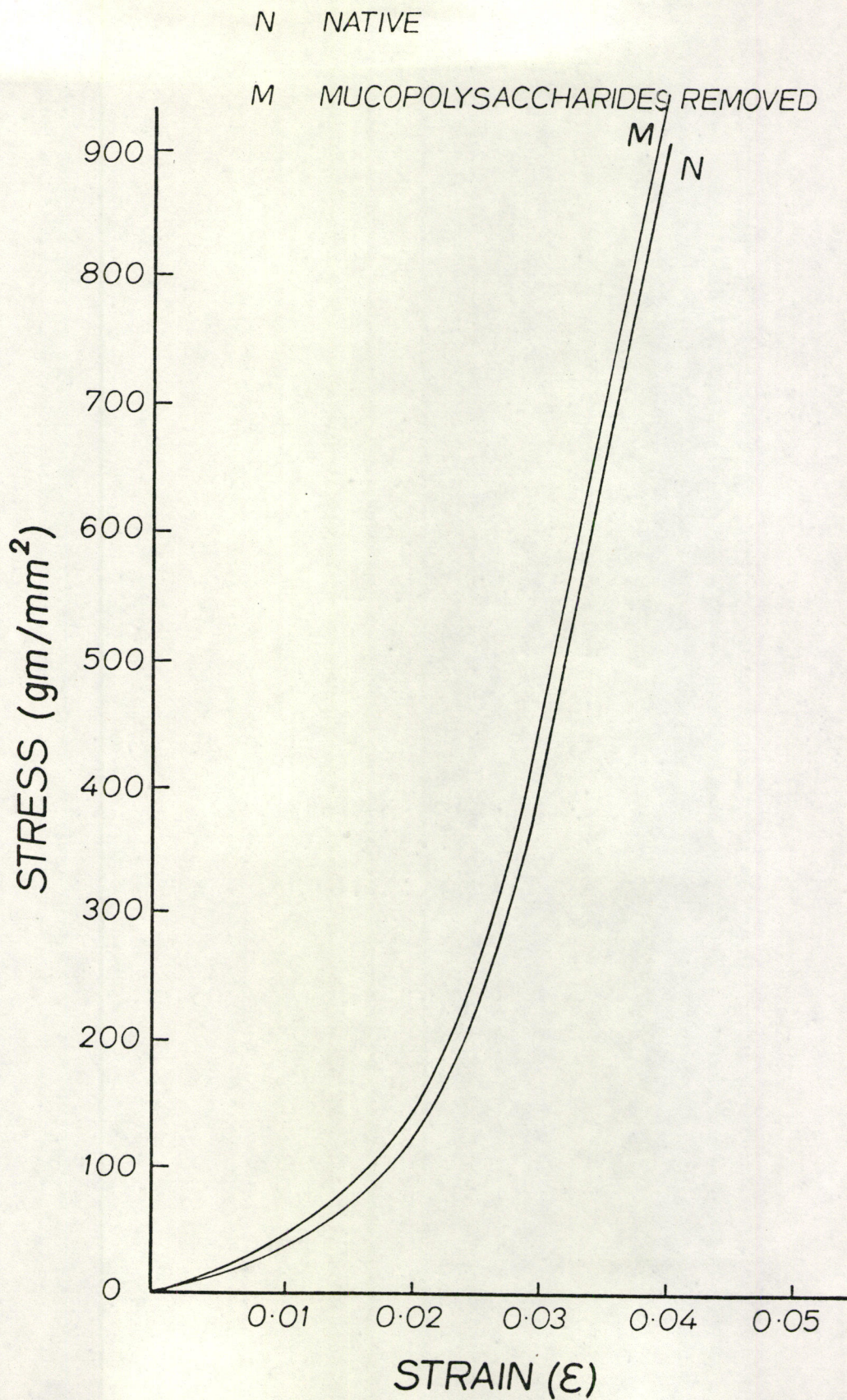


Figure 14: Typical stress-strain curves of dog's Achilles tendon



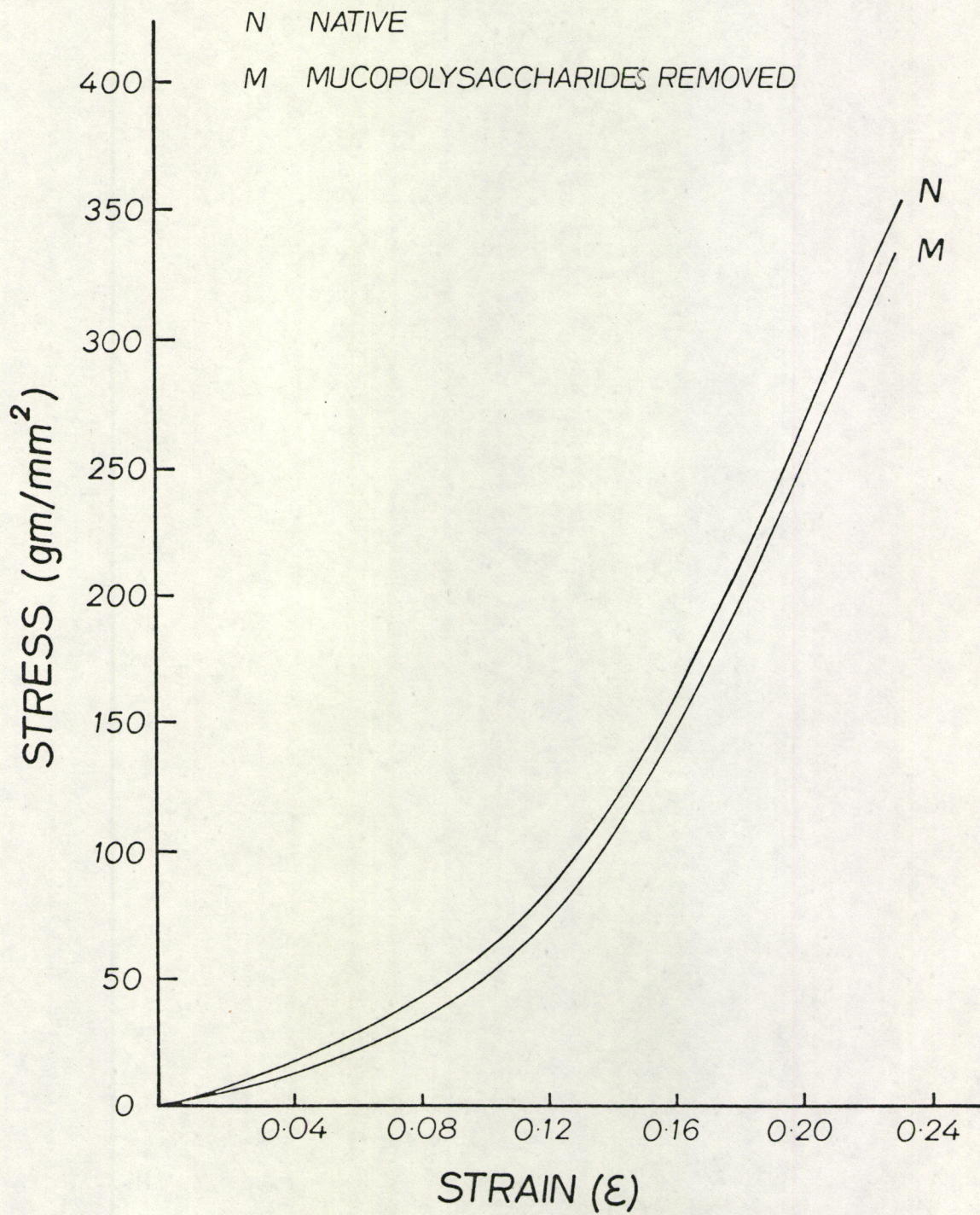


Figure 15: Typical stress-strain curves of dog's cornea



### 3. Contribution of Individual Components

#### Aorta

A basic characteristic of the deformation behaviour of native aortic tissue from the dog, is the appearance of two distinct regions of nearly linear behaviour, one at low extension ( $\epsilon < 0.50$ ) and the other at high extension ( $\epsilon > 0.60$ ). This allows the definition of "low strain" and "high strain" tensile moduli, which are characteristic parameters of each sample over most of its deformation range (Figs. 3, 4, 5, and 6).

Removal of collagen results in an approximately linear response throughout the entire deformation range. The resulting tissue contains elastin and fats and the longitudinal and circumferential moduli are quite similar to the respective low-strain moduli of the native tissue. In a similar manner, the deelasinated samples, which are mainly collagenous, show after an extended initial "toe" region a high modulus, corresponding to the high strain modulus of the native tissue (Table 1 and 2).

An indication of the statistical significance of the measurement is given in Tables 1 and 2 (see also Appendix 2). The effect of the elastin removal is comparatively more significant (to a confidence level of 0.975) in the longitudinal sample of the descending aorta than in the circumferential sample, at low strain. In the case of the ascending aorta, the effect of deelasination is again comparatively more significant ( $P = 0.999$ ) in the longitudinal sample than in the circumferential, at low strain. The high strain moduli in both descending and ascending aorta remain unchanged with deelasination. These tables also reveal directional anisotropy



in the aorta, the anisotropy being highly significant ( $P = 0.999$ ) in the descending aorta at high strain where the circumferential modulus is more than twice the value of the longitudinal modulus.

#### Abdominal Skin

Once again the removal of collagen results in a linear response throughout the entire deformation range with the longitudinal and circumferential moduli being similar to the low-strain moduli of the native tissue.

Table 3 indicates that the effects of elastin removal, at low strain, is highly significant to a confidence level of 0.999 in both the longitudinal and transverse directions. In each case the modulus is reduced by a factor of two. On the other hand, the high-strain moduli in both directions remain unchanged with deelasination. Table 3 also reveals directional anisotropy at low strain where the modulus in the transverse direction is more than three times the value in the longitudinal direction.

#### Achilles Tendon

The low-strain modulus of the native tendon corresponds to the modulus of the decollagenated tissue as shown in Fig. 9.

The effect of elastin removal at low-strain is highly significant ( $P = 0.999$ ) whereby the modulus is reduced by a factor of 3 (Table 4). At high strain, however, the modulus remains essentially unchanged with deelasination.



### Cornea and Sclera

The effect of elastin removal in the cornea, at low strain, results in the modulus being reduced by a factor of three (Table 5) ( $P = 0.999$ ) whereas the high strain modulus remains unchanged. In the sclera the effect of deelastination reduces the modulus by a factor of two at low strain ( $P = 0.999$ ) although at high strain the modulus remains unaffected (Table 6).

#### 4. The Effect of Mucopolysaccharides (MPS) Removal

As can be seen from Figs. 13, 14, 15 the removal of MPS from the ascending aorta, Achilles tendon and cornea respectively does not affect the stress-strain curves of these tissues. This is in agreement with the results published by Hoffman et. al. (20).

#### 5. Explanation of Results

As the descending aorta is one of the main arteries of the body it handles a large volume of blood. It is therefore subjected to high stresses in the circumferential direction. This probably accounts for the higher modulus (at high strain) of the artery in the circumferential direction (Table 1).

The ascending aorta of the dog is extremely short: hardly one inch long with a diameter twice that of the descending aorta. Presumably the function of distribution of blood is handled mainly by the descending aorta. Although it receives the main bulk of the blood from the heart, the wider diameter probably results in a less turbulent flow compared to



the descending aorta. Hence the relatively more isotropic nature of the ascending aorta (Table 2).

From Figs. 7 and 8 it is quite evident that the skin is a highly extensible structure. This is to be expected since the skin is always in a slightly stretched state in vivo and as such it has to be quite elastic (14). A directional variation in extensibility, as is found in human skin, is apparent here (14, 37) (Table 3).

The difference in the results between the aorta and the skin can also be explained in terms of elastic recovery of the tissues. The aorta, being more dynamic than the skin, needs a faster recovery. Hence the native tissue of the aorta has a stress-strain curve with a less extended initial toe region as compared to the skin.

The most striking feature regarding the Achilles tendon of the dog is its extremely high modulus at high strain ( $\approx 60 \text{ kg/mm}^2$ ) (Table 4). Compared with the aorta, say, the difference is certainly tremendous. Nevertheless, if one compares the functions of these tissues, the difference is hardly surprising. The Achilles tendon acts as a force transmitting device in the leg. It is therefore essential that it has fast recovery and is highly collagenous. If tendon is stretched rapidly, high stresses will be induced in it which allows the tendon to effectively transmit large forces to the bones and joints with a relatively small increase in tendon length (1). This accounts for the low elastic limit ( $\approx 4\%$  strain) for the tendon (1). Elliott (11) quotes a tensile strength figure of  $15\text{-}30 \text{ kg/mm}^2$  for mammalian tendon as compared to  $1\text{-}5 \text{ kg/mm}^2$  for the uterus, "a discrepancy which seems too great to be due to the



orientation of the fibres and which implies a difference in the ultimate links of the collagen network" (11). Furthermore, in Abraham's work on the mechanical behaviour of tendon (1), the Young's modulus of human tendon (Fig. 3 of (1)) at 3% strain is found to be approximately  $44 \text{ kg/mm}^2$ . Yamada (46) studied the stress-strain curves of calcaneal tissues of various animals including the dog (Fig. 79 of (46)) and the linear portion of the stress-strain curve of the dog's calcaneal tendon at about 8% strain has a modulus of approximately  $90 \text{ kg/mm}^2$ . So a value of  $60 \text{ kg/mm}^2$  for the dog's Achilles tendon in this report is within reasonable limits.

The sclera forms the posterior four-fifths of the eyeball and is continuous anteriorly with the cornea (7). The sclera consists of dense fibrous tissue arranged in a rather irregular fashion (see section on Histology). The tendons of the extrinsic eye muscles are continued into the sclera in order to provide rotation of the eyeball (7). This means that the sclera needs fast recovery after deformation. Hence the low elastic limit of about 28% (Fig. 12).

The cornea is the transparent anterior continuation of the sclera, and consists of five well-defined layers (7). The layer of interest here is the stroma or substantia propria, constituting the main mass of the cornea. It is continuous with the sclera and consists of very regularly arranged lamellae of collagen fibres (see Histology). In each layer the collagen fibres are parallel with one another, but in adjacent layers the fibres change direction and are roughly at right angles to the fibres in the next layer (7). This explains the high modulus of about  $3000 \text{ gm/mm}^2$  (Table 5) and low elastic limit of about 20% (Fig. 10).



## HISTOLOGY

Extensive histological studies on the various tissues were done at the level of light microscopy in an effort to understand the mechanical behaviour of these tissues from their structural organization.

The tissues were scanned mainly for collagen and elastin utilizing a total of three staining techniques. The tissues were fixed in 10% formalin. They were embedded in paraffin and microtomed to a thickness of 5  $\mu$ . Table 7 indicates the staining techniques along with the identifying colours of the different constituents (30). In general, native, deelasinated and stretched tissues were used for histology. All histological slides were photographed through a microscope using Ektachrome colour film EPY-135.

Figs. 16 and 17 illustrate the respective organization of elastin structures in the longitudinal and circumferential sections of the dog's descending aorta. The elastin appears as well-defined and wavy structures. Figs. 18 and 19 show the organization of collagen in the same two directions. Figs. 16 and 17 indicate that the arrangement of the elastin strands is highly anisotropic, with preferential orientation in the circumferential direction. Similarly Figs. 18 and 19 show preferential orientation of collagen in the circumferential direction. This is in good agreement with the mechanical data. Figs. 20 and 21 show the appearance of the deelasinated descending aorta and the deelasinated ascending aorta where most of the elastin has been removed. The collagenous network appears to be slightly disorganized.

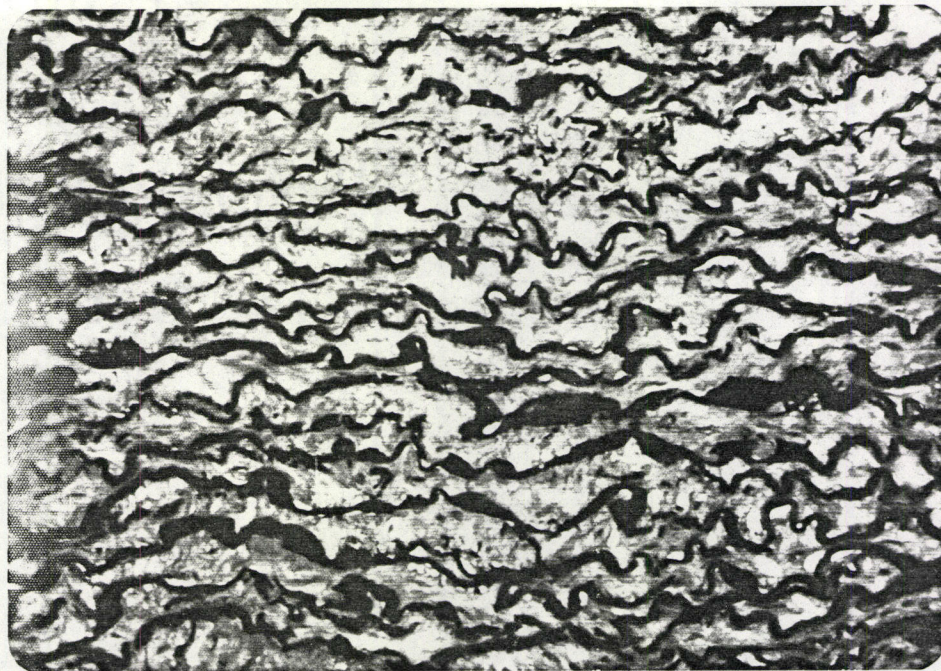


Staining Technique	Collagen	Elastin	MPS	Lipids	Cells
Verhoeff's	Red/Brown	Blue-black	-	-	-
Trichrome	Green	Red	-	-	Reddish, smooth muscle or fibroblasts
Haematoxylin and Eosin (H&E)	red	yellow	-	-	-

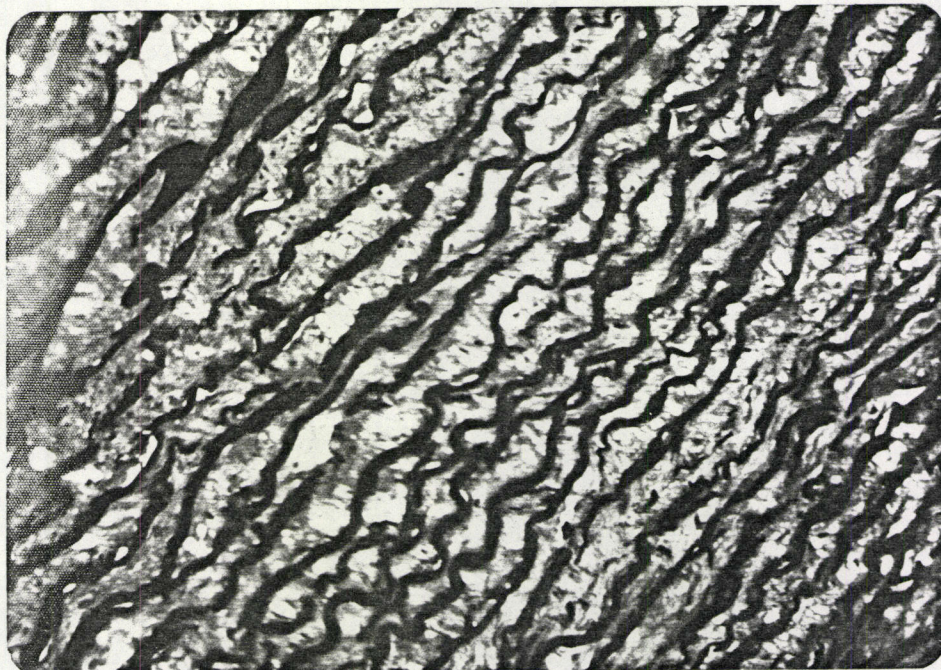
(M.P.S. = Mucopolysaccharides)

TABLE 7: Staining Methods Used in Histology of Dog's Tissues





(16)

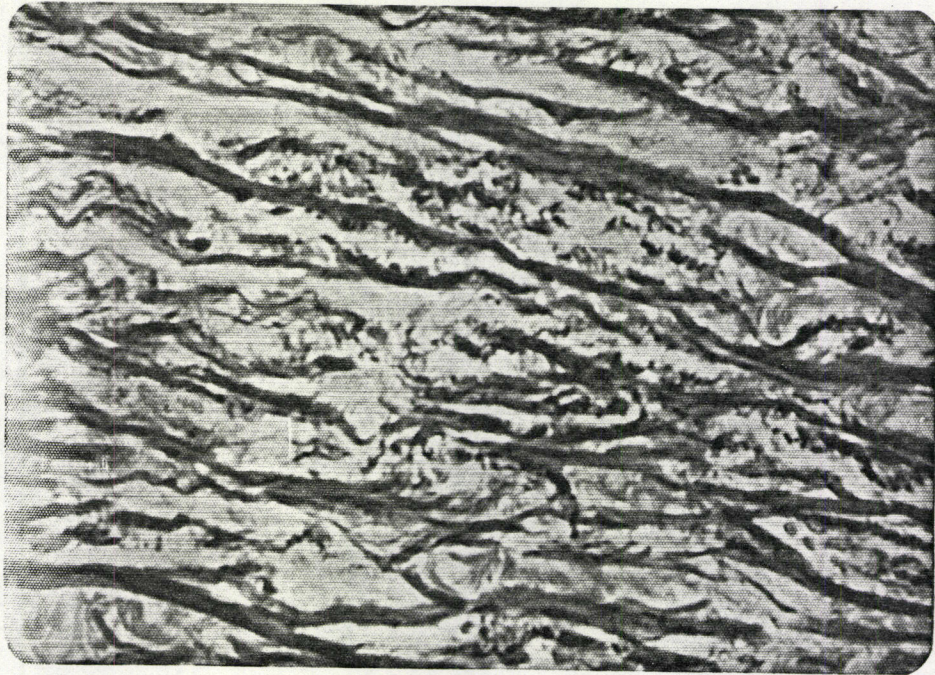


(17)

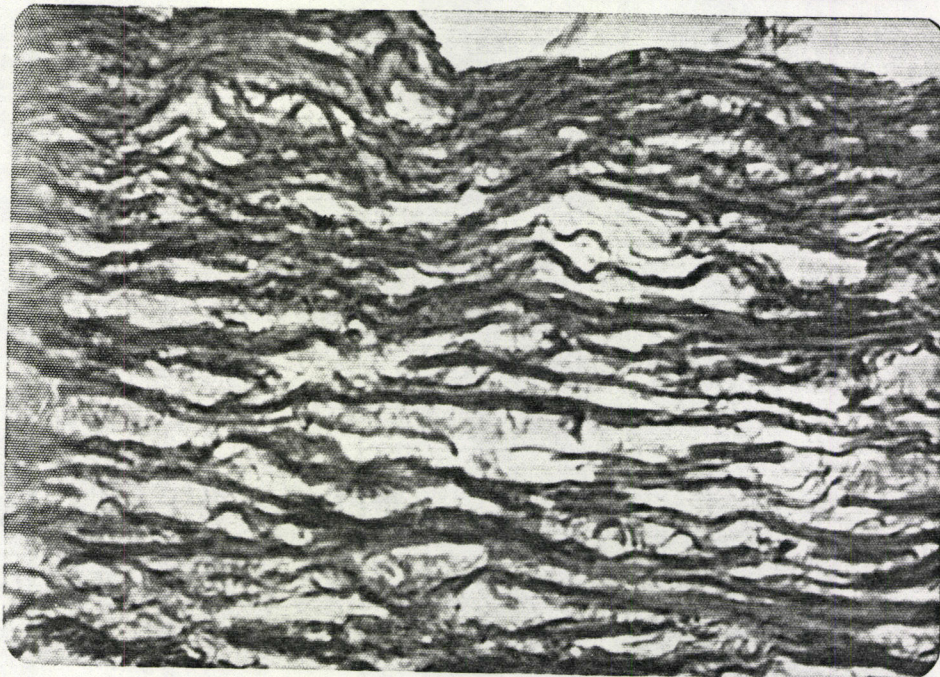
Figure 16: Histological micrograph of native descending aorta. Longitudinal section. Verhoeff's stain (x400).

Figure 17: Histological micrograph of native descending aorta. Circumferential section. Verhoeff's stain (x400)





(18)



(19)

Figure 18: Native descending aorta. Longitudinal section. H&E stain (x400)

Figure 19: Native descending aorta. Circumferential section. H&E stain (x400)





(20)



(21)

Figure 20: Deelastinated descending aorta. Longitudinal section. Verhoeff's stain (x400)

Figure 21: Deelastinated ascending aorta. Longitudinal section. Verhoeff's stain (x400)

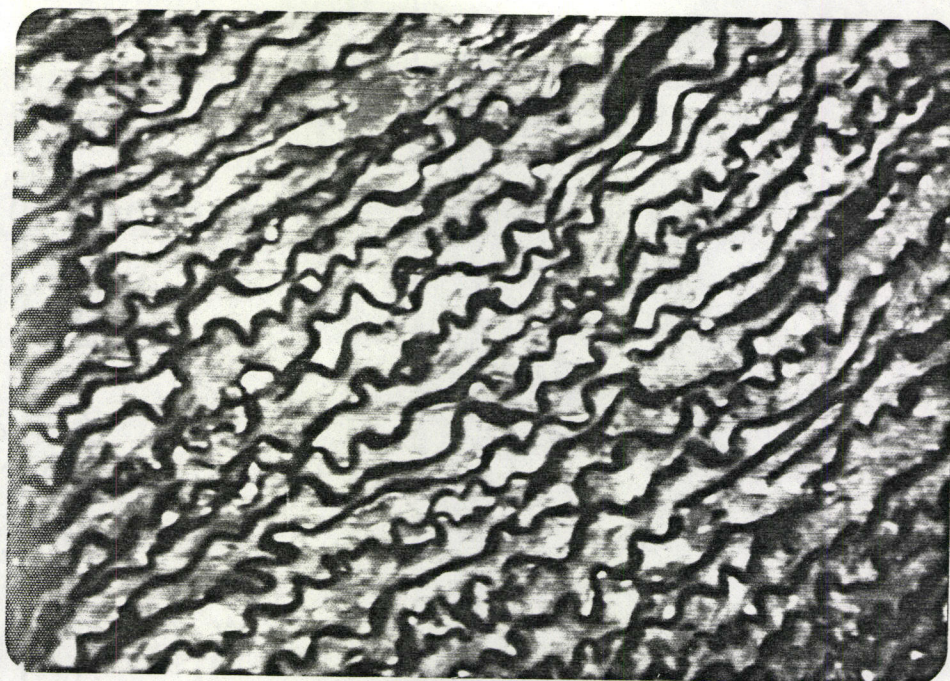


Figures 22 and 23 show the circumferential and longitudinal samples of the ascending aorta in the native state. They do not show directional anisotropy between the circumferential and longitudinal sample. This is consistent with the mechanical data obtained in the stress-strain curve.

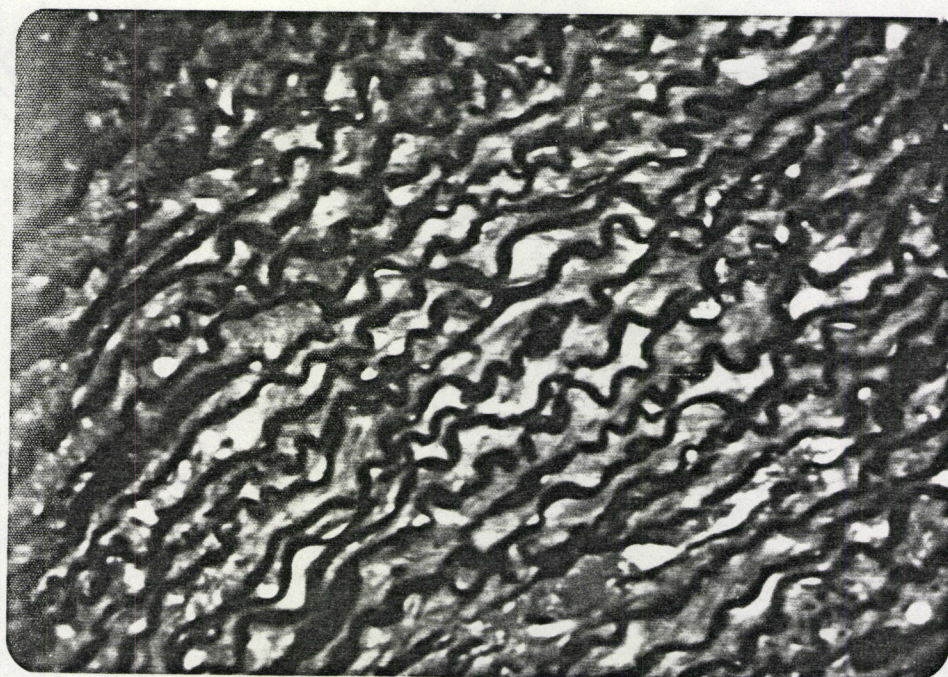
Fig. 24 shows the abdominal skin micrograph in the native state. The elastin fibres are shown to be highly coiled while the collagen seems fragmented. This is probably due to the microtoming and staining technique employed. The highly coiled elastin fibres account for the extended initial toe of the stress-strain curve of this tissue. Fig. 25 shows the deelastinated skin while Fig. 26 gives a much improved micrograph of the deelastinated skin as a result of using the trichrome stain. In the latter figure one could see very clearly the collagenous network and some final traces of elastin.

The Achilles tendon micrograph (Fig. 27) shows a highly oriented, compact, and almost parallel collagen bundles. The use of oil immersion objective (for 1000x magnification) imparts a slightly yellowish colouration to the photograph. The compact arrangement of the collagen bundles is not surprising in view of the high value of Young's modulus obtained in the mechanical test ( $\approx 60 \text{ kg/mm}^2$ ). Elliott (11) attributes this large value of Young's modulus to the high degree of cross-linkage between the collagen fibres of tendon. The micrograph, however, does not show any elastin (see also Project II). This is due to the elastin being obscured by the dense collagen bundles (17). Hass (17) observed a similar masking of elastin by dense collagen bundles in the intimal plaque of the human aorta (see Fig. 2 of (17)).





(22)

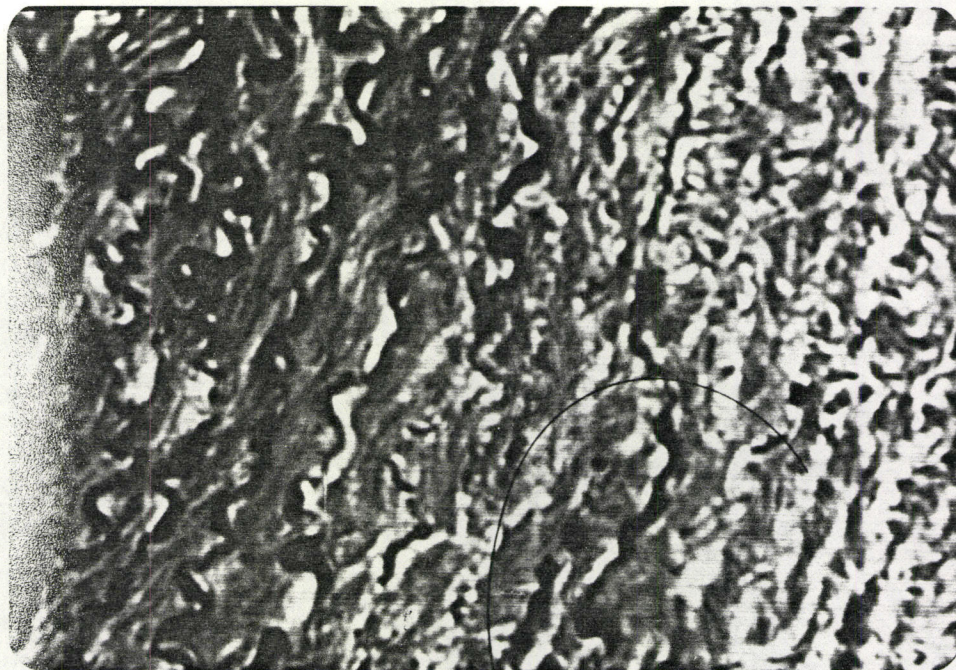


(23)

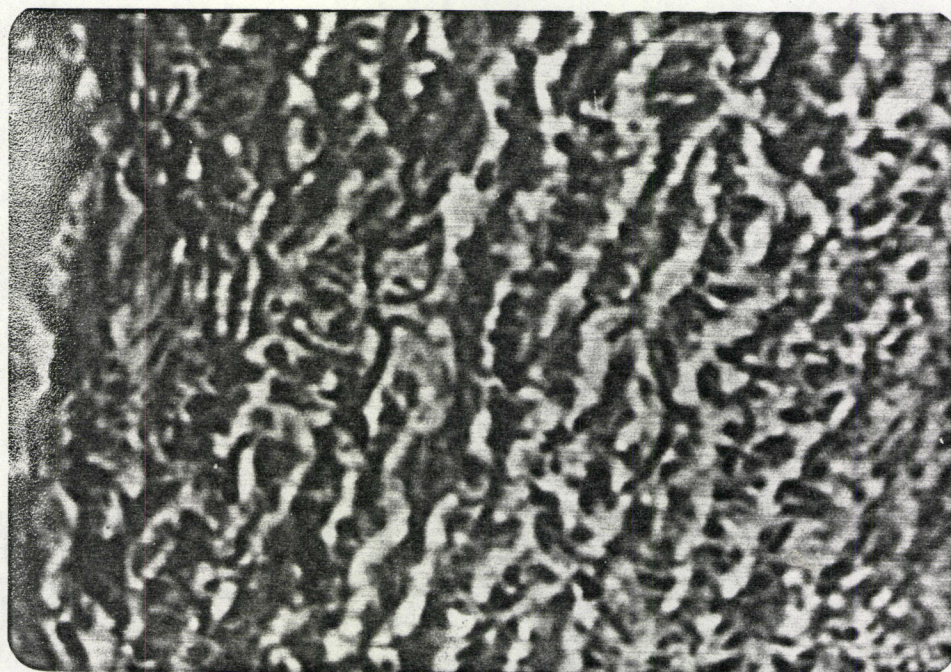
Figure 22: Native ascending aorta. Circumferential sample. Verhoeff's stain (x400)

Figure 23: Native ascending aorta. Longitudinal sample. Verhoeff's stain (x400)





(24)

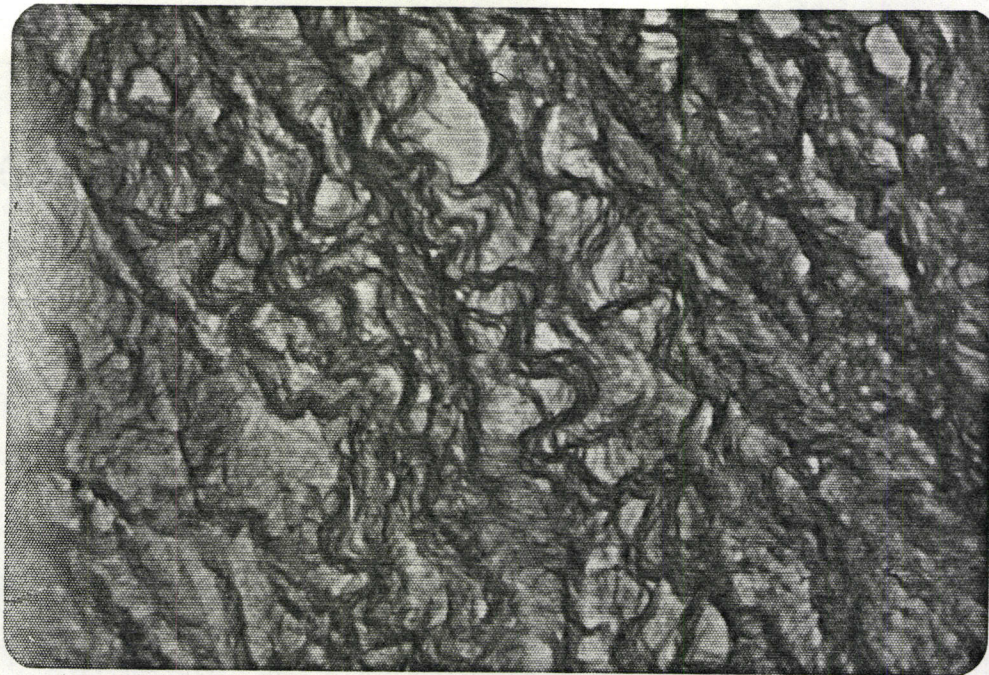


(25)

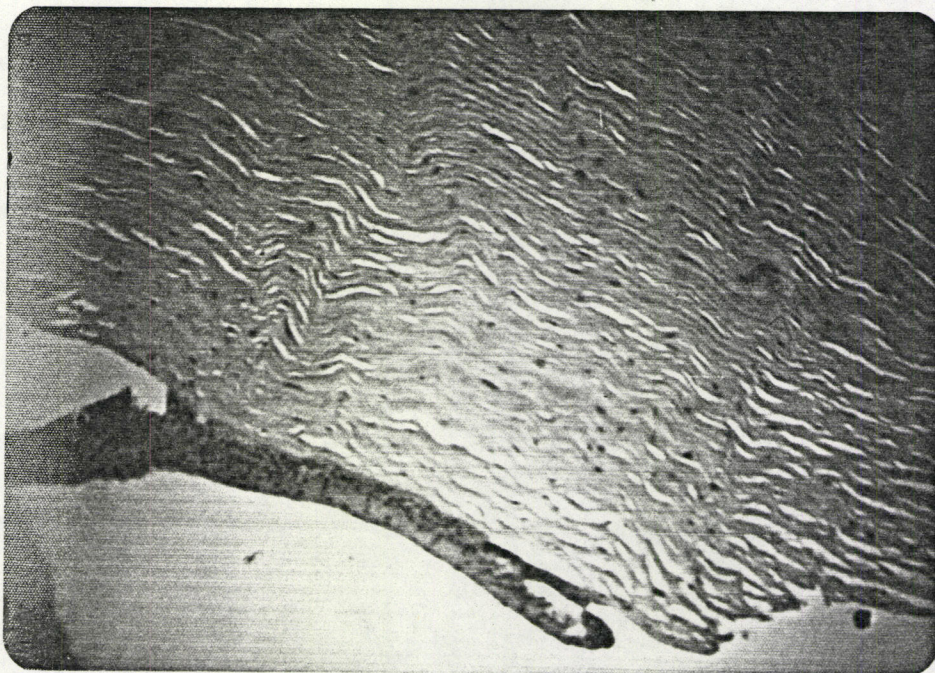
Figure 24: Native abdominal skin. Longitudinal section. Verhoeff's stain (x400).

Figure 25: Deelastinated abdominal skin. Longitudinal section. Verhoeff's stain (x400)





(26)



(27)

Figure 26: Deelasticated abdominal skin. Longitudinal section. Trichrome stain (x400)

Figure 27: Native Achilles tendon. Verhoeff's stain (x1000)



Fig. 28 shows the native cornea as consisting of very regularly arranged lamellae of collagen bundles consistent with the high value of the Young's modulus. On the other hand the collagen fibres in the sclera (Fig. 29) are not as highly organized as in the case of the tendon or cornea. Once again the micrographs for the native cornea and native sclera show no trace of elastin. This is probably due to the same reason as given above for tendon (see also Project II).

#### Histology of Strained Sample

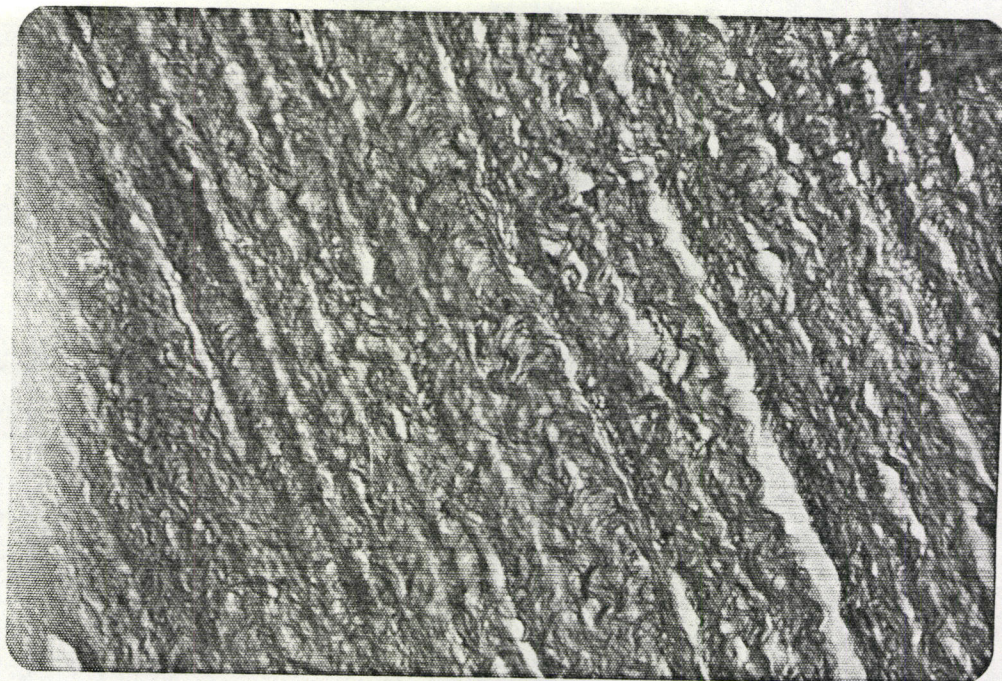
Fig. 30 shows the native descending aorta stretched to 80% ( $\epsilon = 80\%$ ) strain. Here one observes that most of the elastin fibres are straightened out in the direction of stress.

Fig. 31 shows the micrograph for skin stretched to 80% strain. Comparing this figure with Fig. 26 it is evident that most of the waviness of the collagenous network has disappeared - the majority of the fibres are now straightened in the direction of stress. Fig. 32 shows the abdominal skin again, now strained to 150%, whereby the majority of the collagen fibres are now well defined, straight, continuous bundles in the direction of stress. The yellowish patches in Fig. 32 are the elastin network.

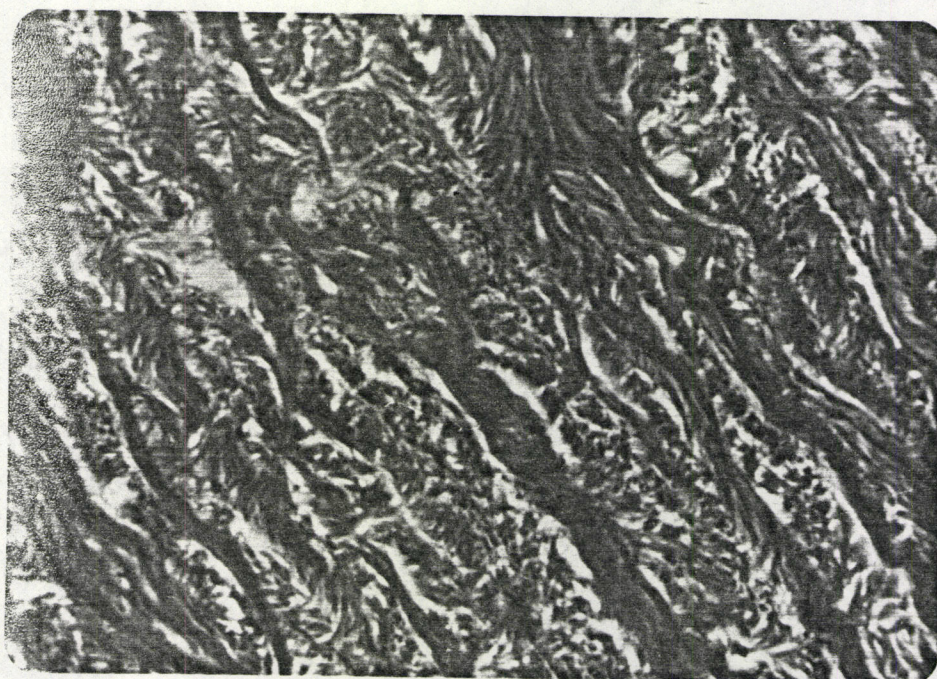
Fig. 33 shows that in the stretched Achilles tendon the collagen bundles become unravelled and most of the waviness seen in the unstressed tendon (Fig. 27) has disappeared. The collagen bundles towards the middle straighten out more than those at the edge of the tendon.

The strained cornea of Fig. 34 reveals that the collagen bundles are now well defined, almost straight continuous bundles in the





(28)

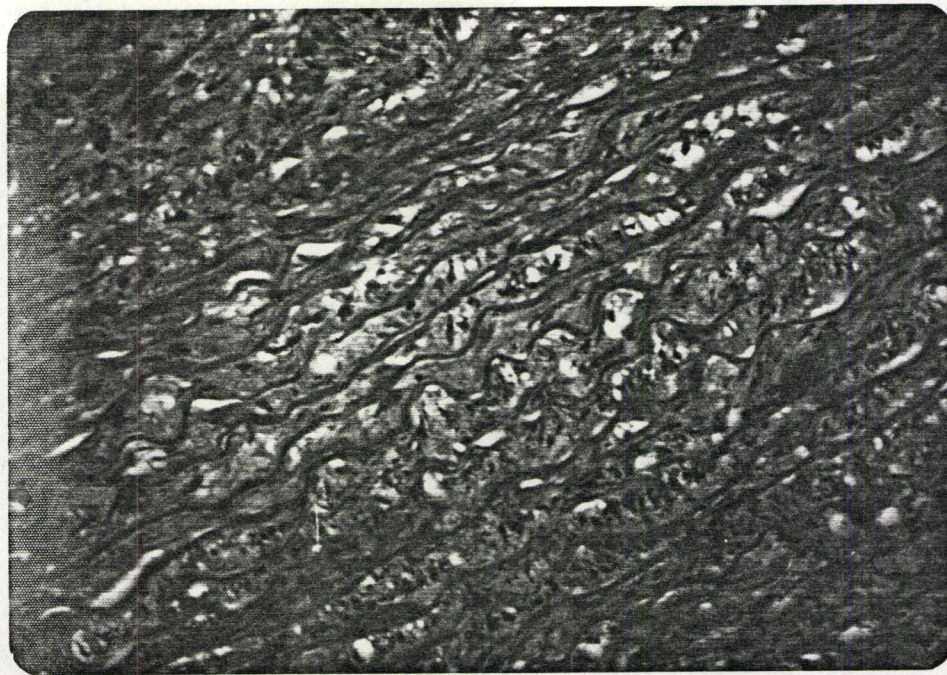


(29)

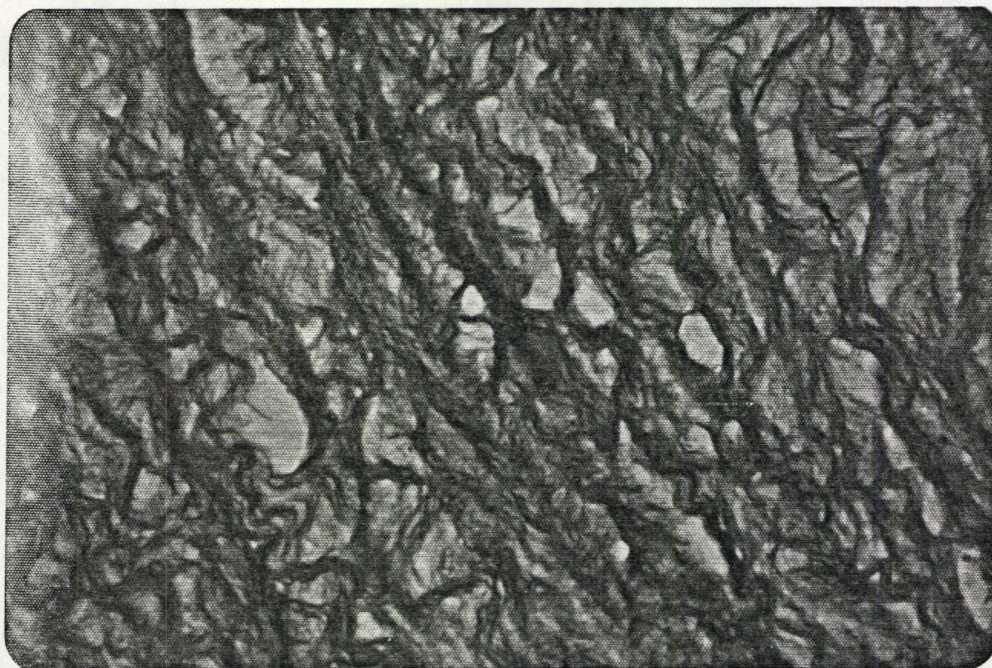
Figure 28: Native cornea. Verhoeff's stain (x400)

Figure 29: Native sclera. Verhoeff's stain (x400)





(30)

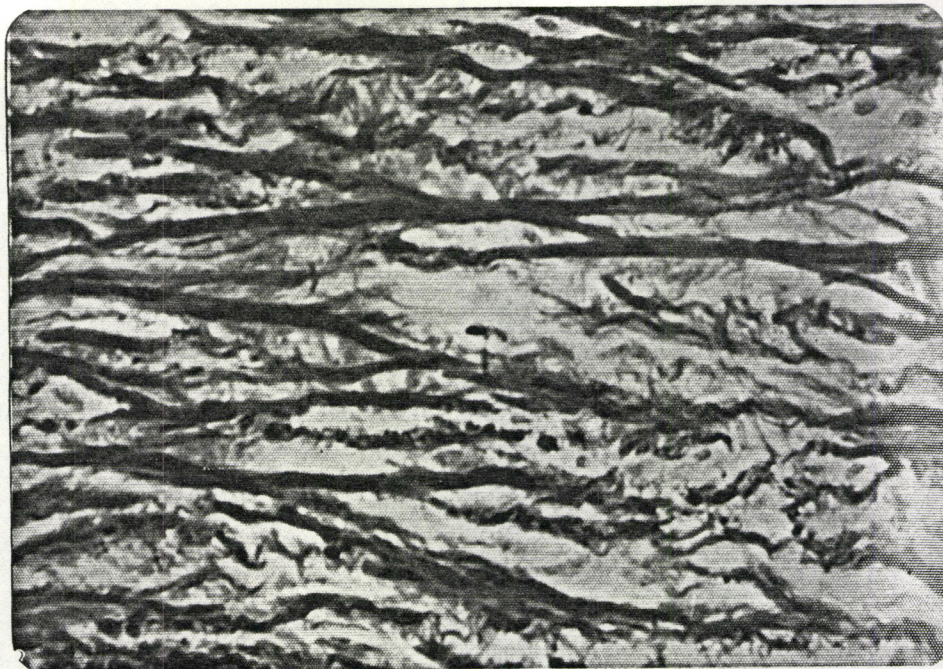


(31)

Figure 30: Strained ( $\epsilon = 80\%$ ) native descending aorta. Circumferential section. Trichrome stain (x400)

Figure 31: Strained ( $\epsilon = 80\%$ ) deelastinated abdominal skin. Longitudinal section. Trichrome stain (x400)





(32)



(33)

Figure 32: Strained ( $\epsilon = 150\%$ ) native abdominal skin. Longitudinal section. H&E stain (x400)

Figure 33: Strained ( $\epsilon = 2\%$ ) native Achilles tendon. Verhoeff's stain (x1000)



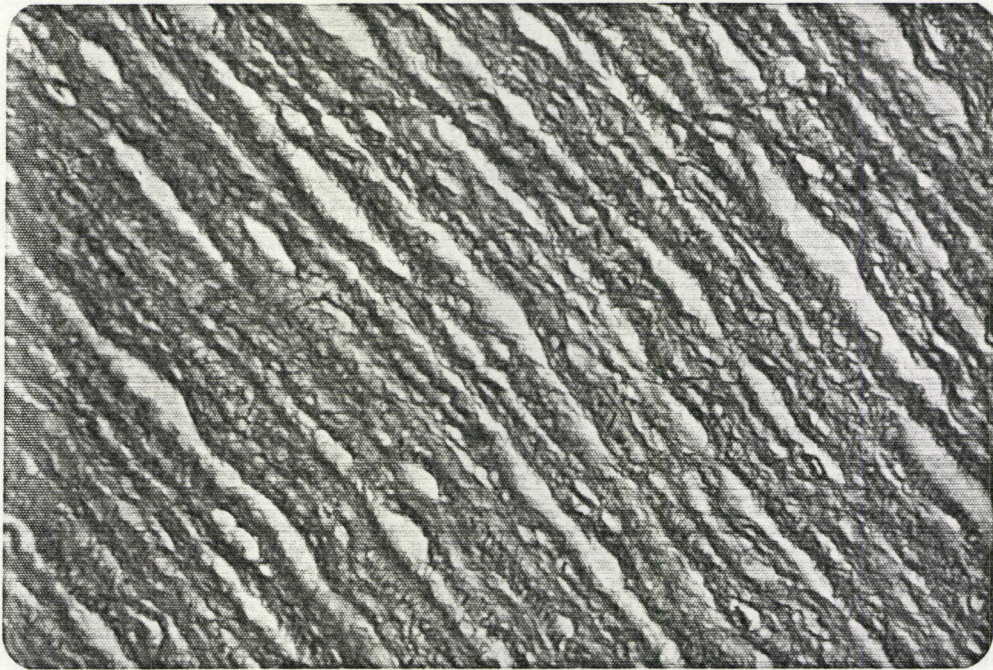


Fig. 34: Strained ( $\epsilon = 20\%$ ) native cornea. Verhoeff's stain (x400)



direction of stress. Comparing with the unstrained cornea (Fig. 28) one can see that the collagen bundles are less compact in the strained cornea.

From the foregoing histology of the strained samples one can conclude that at low extension the stress is borne mainly by the elastin fibres. At high extension, on the other hand, the collagen fibres begin to strain, and, because of their much higher modulus, become the main load-bearing component. This is clearly seen particularly in Fig. 32, where at a strain of 150% the collagen bundles are straightened out in the direction of stress while the elastin appears strained too.



## DISCUSSION

The potential value of the in vitro measurements of the work on the aorta lies in their extrapolation to predict in vivo properties of arterial tissue (24). It is possible to convert the stress-strain data of tensile specimens into corresponding blood-pressure distension values for the whole vessel by means of a relation, developed for the deformation of pressurized isotropic tubes with fixed ends (24). The expression requires knowledge of the thickness-to-diameter ratio of the tube and Poisson's ratio of the material (43). Despite the known anisotropy of aortic tissue and its unknown Poisson's ratio, this conversion is often made (35).

Yamada (46) studied the stress-strain characteristic of the dog's thoracic aorta in the native state. The slope of his stress-strain curve at 110% elongation in the circumferential direction gives a modulus of  $300 \text{ gm/mm}^2$  whereas in this report a corresponding value of  $737.8 (\pm 67.39) \text{ gm/mm}^2$  at 52% elongation is obtained for the descending aorta. In the longitudinal direction, Yamada's (46) typical stress-strain curve gives a modulus of  $230 \text{ gm/mm}^2$  at 100% elongation as compared to a modulus of  $353.9 (\pm 63.57) \text{ gm/mm}^2$  at 55% strain obtained in this report. Yamada's (46) figures for the circumferential and longitudinal moduli show a slight anisotropy whereas the moduli for the descending aorta in this report show a pronounced anisotropy; the circumferential modulus being twice that of the longitudinal. One possible explanation of the discrepancy could be that the descending aorta used in this report might have been diseased



or aged since Learoyd and Taylor (27) and Mack (28) observed a rise in Young's modulus due to aging and arteriosclerosis in the human arterial tissue. Patel et. al. (35) studied the static anisotropic elastic properties of the middle descending thoracic aorta of living dogs and found that at a physiologic pressure of 154 cm H<sub>2</sub>O (at a strain of 52%) the mean values of the elastic moduli (in vivo) in the circumferential and longitudinal directions were 75.10 and 101 gm/mm<sup>2</sup> respectively; and the longitudinal modulus was found to decrease by 32% when the vessel was studied in vitro due to the loss of normal tethering of the blood vessel in situ (35). Again the moduli values from Patel et al's (35) show a directional anisotropy which is not as pronounced as that obtained in this report.

Yamada (46) determined the ultimate tensile strength of the dog's ascending aorta in the circumferential direction to be 70 gm/mm<sup>2</sup> and its ultimate percentage elongation to be 145%. Furthermore, this work shows no directional anisotropy in the ascending aorta of the dog. As explained earlier this is probably related to size and function. The ascending aorta of the dog has a diameter which is more than twice that of the descending aorta. Consequently the flow of blood in this vessel is less turbulent compared to the flow in the narrower descending aorta. Hence the isotropic nature of the ascending aorta.

Yamada (46) studied the stress-strain characteristics of dog's abdominal skin (in the native state) in the circumferential (transverse) and longitudinal directions. The slopes of his stress-strain curves give a modulus of 1333 gm/mm<sup>2</sup> (at 150% strain) in the transverse direction as compared to a corresponding value of 1909 gm/mm<sup>2</sup> in this report; and a



modulus of  $1842 \text{ gm/mm}^2$  (at 160% strain) in the longitudinal direction as compared to a corresponding value of  $1875 \text{ gm/mm}^2$  in this work. Evidently the figures in these two agree closely. Kenedi et. al. (21) made a similar study on human skin in vitro and showed that the stress-strain curves consist of two regions - a primary range showing large extensions for low loads as obtained in this report and by Yamada (46); and a "secondary" stage during which the increments of extension continue to decrease with increasing load, again as obtained in this report. Kenedi et. al. (21) also postulated that the curves may be represented by the relationship  $\sigma = A\epsilon^n$  where A and n are coefficients obtained from experimental results. Ridge and Wright (37), in their tests on human skin, also express their results in power form. The main effect of age, according to Kenedi et. al. (21), appears to be a less extended primary range with increasing age. Kenedi et. al. (21) also found the abdominal skin in the direction of the longitudinal axis of the body to be more extensible at low loads than in the circumferential direction. This phenomenon is evident in this report in which the mean value of the Young's modulus of the native skin at low strain ( $\epsilon = 40\%$ ) is higher in the circumferential direction ( $87.50 \text{ gm/mm}^2$ ) than in the longitudinal ( $25.0 \text{ gm/mm}^2$ ) direction.

The Young's modulus of the dog's Achilles tendon as obtained in this report is  $60 \text{ kg/mm}^2$  at 3.5% strain. Abrahams (1) studied the stress-strain characteristics of human Achilles tendon and horse extensor tendon and from Fig. 3 of (1), the Young's modulus of the Achilles tendon of a 54-year-old woman, is calculated to be  $44 \text{ kg/mm}^2$  ( $\epsilon = 3.5\%$ ) approximately. The modulus as obtained from the stress-strain curve of the dog's calcaneal



tendon (46) is approximately  $90 \text{ kg/mm}^2$  at 8% strain. Elliott (11) indicates that there exists considerable variation in the estimates of tensile strength of tendon not only between different authors but within any one investigation, and this may be attributed to either experimental error or to a real variation in the tensile strength relative to the collagen present (11). The latter could be due to variation of the cohesion between the collagen fibres, to variation of the molecular orientation within the tendon or, by analogy with the difference between stress-strain curves of nylon thread and nylon stockings, to some variation of the interweaving of the fibres (11). The highest stress subjected on the Achilles tendon in this work is around  $900 \text{ gm/mm}^2$ . A further source of variations between the estimates of tensile strength (and hence Young's modulus) could lie in the collagen itself (11). Expressed in terms of the collagen present, tensile strength range from  $15\text{-}30 \text{ kg/mm}^2$  for tendons to  $1\text{-}5 \text{ kg/mm}^2$  for the uterus and other tissues, "a discrepancy which seems too great to be due to the orientation of the fibres and which implies a difference in the ultimate links of the collagen network" (11). Van Brocklin and Ellis (44) determined the stress strain curve of human extensor digitorum tendon and the slope of the stress-strain curve of Fig. 5 of (44) gives a modulus of  $87.5 \text{ kg/mm}^2$  ( $\epsilon = 2.5\%$ ) approximately. In the light of the moduli values of human and dog's tendon from various parts of the body quoted above, a figure of  $60 \text{ kg/mm}^2$  for the modulus of the dog's Achilles tendon seems reasonable.

To the best of the author's knowledge the only work done on the mechanical properties of the dog's cornea and sclera are those by Yamada (46) where he studied the stress-strain and pressure-expansion curves of



human and animal's cornea and sclera including the dog's. He (46) drew typical stress-strain curve for the dog's cornea from which the slope is found to be  $3600 \text{ gm/mm}^2$  at 20% strain although he did not specify whether the curve is for the meridional or equatorial section of the cornea. In this report a mean modulus of  $2953.4 \text{ gm/mm}^2$  at 20% strain is obtained for the meridional section of the cornea. Yamada (46) also obtained an ultimate tensile strength figure of  $410 \text{ gm/mm}^2$  at an ultimate percentage elongation of 23.3% strain. Nevertheless, the Young's modulus figure obtained here is reliable enough considering the uncertainty in Yamada's data.

In this report a mean Young's modulus of  $5445.2 \text{ gm/mm}^2$  is obtained for the meridional section of the dog's sclera at 22% strain in the native state; Yamada's (46) stress-strain curve for the meridional section of the dog's sclera gives a slope (i.e. Young's modulus) of  $6000 \text{ gm/mm}^2$  at the same strain of 22%. From Fig. 223 of Yamada (46) the meridional section of the sclera has an ultimate tensile stress of about  $960 \text{ gm/mm}^2$  (as compared to a range of  $700\text{-}900 \text{ gm/mm}^2$  being the maximum stress value subjected to the sclera in this work) at an ultimate percentage elongation of 27% (as compared to a maximum strain of about 26% in this report).

At this point one may very well ask the question: "Why is there such a large variation in the Young's modulus values of the various tissues; for instance a modulus of  $100 \text{ gm/mm}^2$  for the ascending aorta as contrasted to a figure of  $60 \text{ kg/mm}^2$  for the Achilles tendon both at high strain?" The answer to this question is well summarised by Elliott (11) in his work on the "Structure and Function of Mammalian Tendon" which is quoted here:



"Expressed in terms of the collagen present, tensile strength (and hence Young's modulus) ranges from 15-30 kg/mm<sup>2</sup> for tendons to 1-5 kg/mm<sup>2</sup> for the uterus and other tissues, a discrepancy which seems too great to be due to the orientation of the fibres and which implies a difference in the ultimate links of the collagen network". Another explanation for the variation in modulus between the various tissues is related to the function of the particular tissue. This has already been discussed in some detail in the sections "Structure" and "Explanation of Results" in this report.

In this report no studies are carried out to determine the effect of strain rate on the behaviour of the stress-strain curves of the tissues. Rigby et. al. (38) reported that increase in the rate of strain of rat tail tendons did not alter significantly the shape of the stress-strain curve. The main effect was an increase in the load required to produce a given strain. Missirlis (30) studied the effect of strain rate on the elastic modulus of aortic valve tissue and reported that an increase in the rate of strain over a two and a half decades range did not affect the elastic modulus of the collagenous structure of the tissue i.e. the high strain modulus remains essentially unchanged. In this work a constant cross head speed of 2 mm/min was used for all the tissues.

The removal of elastin results in a reduction in the moduli of the tissues at low strain although the high strain moduli remain essentially unchanged. This is in agreement with the work of Lake (24) and Missirlis (30). It also proves that the enzymolysis technique used destroys only the elastin leaving the collagen intact. The removal of collagen results



in a linear response with moduli comparable to the low-strain moduli of the respective native tissues. At high strain the removal of collagen is highly significant for all the tissues studied. The removal of MPS does not affect the stress-strain curves of the ascending aorta, Achilles tendon, and cornea. This is in agreement with the work of Hoffman et. al. (20). This indicates that the MPS constitute a very small percentage of the whole tissue (see Project II) and acts only as a matrix in which the various tissue constituents are embedded.

Throughout this work attempts have been made to correlate the stress-strain characteristics of the tissues with histology. This has been successful in the cases of the aorta and abdominal skin only. Although the stress-strain curves of the Achilles tendon, cornea and sclera indicate the presence of elastin, histology proves otherwise (see also Project II). This is probably due to the dense and closely packed collagenous network in these tissues masking the elastin. Hass (17) observed a similar phenomenon in the intimal plaque of the human aorta which in the intact aorta was composed principally of dense bundles of collagen. On removal of the collagen by extraction, the residual structure of the sclerotic plaque persisted in the form of a system of delicate elastic networks as shown in Fig. 2 of (17) (see also Project II).

One practical use of this work is in the definition of a "normal" tissue to serve as a criteria for homograft or heterograft quality or to provide a contrast with diseased tissue. Sumner et. al. (42) measured the stress-strain characteristics of aneurysms and compared them with the non-aneurysmic portions of the same vessels in order to correlate



with the greater rigidity of the aneurysmic segments. This work can provide the basis for the design of prosthetic devices. For the latter purpose another important information needed is the porosity content of the various tissues. This is the subject of Project II.



#### SUMMARY OF CONCLUSIONS

1. Collagen and elastin are the main structural components of the dog's native tissues. They exhibit collagen-like behaviour at high strains and elastin-like behaviour at low strains.
2. The descending aorta exhibits directional anisotropy between the longitudinal and circumferential samples.
3. The enzymolysis technique used for the removal of elastin destroys most of the elastin but leaves the collagen intact.
4. The removal of MPS in the ascending aorta, Achilles tendon, and the cornea does not affect the stress-strain characteristics of these tissues.
5. Histological observations, to a large extent, agree with and help explain the previous conclusions.



## REFERENCES

1. Abrahams, M., "Mechanical Behaviour of Tendon in Vitro". Medical and Biological Engineering, 5, pp. 433-443: 1967.
2. Apter, Julia T., "Mathematical Development of a Physical Model of Some Visco-elastic Properties of the Aorta". Bulletin of Mathematical Biophysics, 26, pp. 367-388: 1964.
3. Apter, J.T. and Marquez, Elsa, "A Relation Between Hysteresis and Other Viscoelastic Properties of Some Biomaterials". Biorheology, 5, pp. 285-301: 1968.
4. Apter, Julia T.; Rabinowitz, Murray; Cummings, Dorothy H., and Marquez, Elsa, "Correlation of Viscoelastic Properties with Macroscopic Structure of Large Arteries". Circulation Research XIX, pp. 104-121: 1966, XXI, pp. 901-918: 1967, and XXII, pp. 393-404: 1968.
5. Barratt-Boyes, B.G., "Homograft Replacement for Aortic Valve Disease". Modern Concepts of Cardiovascular Disease, 36, pp. 1-6: 1967.
6. Bergel, D.H., "The Visco-Elastic Properties of the Arterial Wall". Ph.D. Thesis, University of London, 1960.
7. Bloom, William and Fawcett, Don W., A Textbook of Histology, 9th Ed. W.B. Saunders Co., Philadelphia: 1968.
8. Burton, Allan C., "Relation of Structure to Function of the Tissues of the Wall of Blood Vessels". Physiological Reviews, 34, pp. 619-642: 1954.
9. Carpentier, Alain; Lemaigre, Guy; Robert, Ladislav, Carpentier, Sophie; Dubost, Charles, "Biological Factors Affecting Long-Term Results of Valvular Heterografts". Journal of Thoracic and Cardiovascular Surgery, 58, pp. 467-483: 1969.
10. Eldon, H.R., "Hydration of Connective Tissue and Tendon Elasticity". Biochim. Biophys. Acta, 79, pp. 592-599: 1966.
11. Elliott, D.H., "Structure and Function of Mammalian Tendon", Biological Review, 40, pp. 392-421: 1965.
12. Finlay, B., "Dynamic Mechanical Testing of Human Skin in Vivo". J. of Biomech., 3, pp. 557-568: 1970.



13. Fung, Y.C.B., "Elasticity of Soft Tissue in Simple Elongation". American Journal of Physiology, 213, pp. 1532-1544: 1967.
14. Gibson, T.; Stark, H. and Evans, J.H., "Directional Variations in Extensibility of Human Skin in Vitro". J. of Biomechanics, 2 pp. 201-204: 1969.
15. Gou, Perng-Fii, "Strain Energy Function for Biological Tissues". Journal of Biomechanics, 3, pp. 547-550: 1970.
16. Gow, Barry S., and Taylor, Michael G., "Measurement of Viscoelastic Properties of Arteries in the Living Dog". Circulation Research, XXIII, pp. 111-122: 1968.
17. Hass, George M., "Elastic Tissue I and II". Archives of Pathology, 34, pp. 807-819: 1942.
18. Hass, George M., "Elastic Tissue I and II". Archives of Pathology, 34, pp. 971-981: 1942.
19. Haas, George M., "Elastic Tissue III:.". Archives of Pathology, 35, pp. 29-48: 1943.
20. Hoffman, A.S.; Granda, L.A.; Gibson, P.; Park, J.B.; Daly, C.H.; Bornstein, P., and Ross, R., "Preliminary Studies on Mechanochemical-Structure Relationships in Connective Tissues Using Enzymolysis Technique". In Perspectives in Biomedical Engineering, Ed. by R.M. Kenedi, The MacMillan Press Ltd., London, 1971.
21. Kenedi, R.M.; Gibson, T.; and Daly, C.H., "Bioengineering Studies of the Human Skin - II". Proc. Symp. on Biomech. and Related Bio-Eng. Topics (Ed. by R.M. Kenedi), pp. 147-158: Pergamon Press, Oxford: 1964.
22. Kramsch, D., "The Protein and Lipid Composition of Arterial Elastin in Aging and Atherosclerosis". Experimental Gerontology, 4, pp. 1-6: 1969.
23. Krokosky, E.M., and Kronskop, T., "Synthetic Aortas for Systemic Simulators". Journal of Biomedical Materials Research, 2, pp. 357-375: 1968.
24. Lake, Larry W., "Structure-Property Relations of the Aortic Wall and its Tissue Constituents". Ph.D. Thesis, Rice University, Texas: 1973.
25. Lawton, Richard, W., "Measurements on the Elasticity and Damping of Isolated Aortic Strips of the Dog". Circulation Research, III, pp. 403-408: 1955.



26. Lawton, Richard, W., "Variability of the Viscoelastic Constants Along the Aortic Axis of the Dog". Circulation Research, VIII, pp. 381-389: 1960.
27. Learoyd, Brian, M., and Taylor, Michael G., "Alterations With Age in the Viscoelastic Properties of Human Arterial Walls". Circulation Research XVIII, pp. 278-292: 1966
28. Mack, G.; Ebel, A.; Kempf, E.E.; Pantesco, V.; Fontaine, J.L., and Fontaine, R., "Aortic Aging and its Connection with Arteriosclerosis, Experimental Results". Journal of Cardiovascular Surgery (Torino), 11, pp. 292-296: 1968.
29. Middleman, Stanley, Transport Phenomena in the Cardiovascular System. Wiley-Interscience, Inc., New York, 1971 .
30. Missirlis, Y.F., "In Vitro Studies of Human Aortic Valve Mechanics". Ph.D. Thesis Rice University: 1973.
31. North, J.F., "Impact Characteristics of Human Skin and Subcutaneous Tissues". Thesis, Bioengineering Unit, University of Strathclyde, Glasgow, Scotland: 1972.
32. Partington, F.R. and Wood, G.C., "The Role of Noncollagen Components in the Mechanical Behaviour of Tendon Fibres". Biochem. biophys. Acta, 69, pp. 485-495: 1963.
33. Partridge, S.M., "Elastin". In "Advances in Protein Chemistry" 17, pp. 227-302. Academic Press, New York, 1962.
34. Patel, Dali J.; Tucker, William K.; and Janicki, Joseph S., "Dynamic Elastic Properties of the Aorta in the Radial Direction". Journal of Applied Physiology, 28, No. 5, pp. 578-582: 1970.
35. Patel, Dali J.; Janicki, Joseph S.; and Carew, Thomas E., "Static Anisotropic Elastic Properties of the Aorta in Living Dogs". Circulation Research XXV, pp. 765-779: 1969.
36. Peterson, Lysle H.; Jensen, Roderick E., and Parnell, J., "Mechanical Properties of Arteries in Vivo". Circulation Research, VIII, pp. 622-639: 1963.
37. Ridge, M.D. and Wright, V., "The Directional Effects of Skin". Journal of Investigative Dermatology, 46, pp. 341-346: 1966.
38. Rigby, B.J.; Hirai, N.; Spikes, J.D; and Eyring, H., "The Mechanical Properties of Rat Tail Tendon". Journal of General Physiology, 43, pp. 265-283: 1959.



39. Rigby, B.J., "Effect of Cyclic Extension on the Physical Properties of Tendon Collagen and its Possible Relation to Biological Aging of Collagen". Nature, London, 202, pp. 1072-1074: 1964.
40. Ross, Donald; and Yacoub, Magdi H., "Homograft Replacement of the Aortic Valve, A Critical Review". Progress in Cardiovascular Diseases, 11, pp. 275-293: 1969.
41. Roy, Charles S., "Elastic Properties of the Arterial Wall". Journal of Physiology, 3, pp. 125-159: 1880.
42. Summer, D.S.; Hokanson, D.E.; and Strandess, D.E.; "Stress-Strain Characteristic and Collagen/Elastin Content of Abdominal Aortic Aneurysms". Surgery, Gynaecology and Obstetrics, 130, pp. 459-466: 1970.
43. Timoshenko, S., and Goodier, J.N., Theory of Elasticity, Wiley, New York, 1951: pp. 258.
44. VanBrocklin, J.D., and Ellis, D.G., "A Study of the Mechanical Behaviour of Toe Extensor Tendons Under Applied Stress". Archs. Phys. Med. Rehab., 46, pp. 369-373: 1965.
45. Wolinsky, Harvey, "Response of the Rat Aortic Media to Hypertension". Circulation Research, XIV, pp. 400-413: 1964.
46. Yamada, Hiroshi, Strength of Biological Materials. Robert E. Krieger Publishing Company, Huntington, New York: 1973 (Ed. by F. Gaynor Evans).
- 47a. Yannas, I.V.; and Huang, C., "Mechanochemical Studies of Enzymatic Degradation of Insoluble Collagen Fibres". J. Biomed. Mater. Res. Symposium, #8, pp. 137-154: 1977.
- 47b. Yannas, I.V.; Burke, J.F.; Huang, C.; and Gordon, P.L., "Correlation of in vivo Collagen Degradation with in vitro Measurements", J. Biomed. Mater. Res., 9, pp. 623-628: 1975.



## APPENDIX 1

### The Concept of Stress and Strain In Biological Materials

Many materials, for example, metals, deform when a force is applied and, provided the force has not been too great, return to their original shape when unloaded. Such perfectly elastic materials generally show a linear relation between the applied force and the deformation and are often referred to as Hookean solids. The constants in the force-deformation relationships are the elastic constants or moduli of the material. The moduli relate stress and strain. Stress is the applied force per unit area and strain is the resulting relative deformation. If the strains are very small (infinitesimal) the deformations may be related to the original unstressed dimensions. Thus, in considering linear, tensile strains, as in a wire,

stress  $\sigma = F/A$ , where  $F$  = force;  $A$  = cross-sectional area;

strain  $\epsilon = \Delta l/l$ , where  $\Delta l$  = incremental length;  $l$  = original length;

and the tensile or Young's modulus of elasticity  $E = \sigma/\epsilon$

Similarly, we may define the bulk modulus  $K$ , relating volume changes to hydrostatic compressive forces and the shear modulus  $G$ , relating shear stress to shear strain.

Stresses applied to a body may be resolved into components along the three principal axes. For a simple isotropic material the relation between stress and strain will be the same in any direction. Such a material may also be homogeneous that is, of uniform structure.



A primary strain produced in a material will set up secondary strains, thus a stretched wire will show changes in radius and total volume. If the initial dimensions of the specimen are  $l$ ,  $a$ ,  $b$ , then a change in  $l$  gives a strain

$$\epsilon_1 = \Delta l/l \quad (1)$$

$$\epsilon_2 = \Delta a/a = -\mu_2 \epsilon_1 \quad (2)$$

$$\epsilon_3 = \Delta b/b = -\mu_3 \epsilon_1 \quad (3)$$

The ratio between strains,  $\mu$ , is termed Poisson's ratio. There are six independent Poisson's ratio corresponding to primary strains in the  $l$ ,  $a$ , and  $b$  dimensions. If the material is isotropic these are all equal.

It can be shown that for an isotropic material two elastic constants suffice to describe its properties and that the three elastic moduli and  $\mu$  are interrelated (6). Thus

$$K = \frac{2(1 + \mu)}{3(1 - 2\mu)} \quad G = \frac{E}{3(1 - 2\mu)} \quad (4)$$

$$G = \frac{E}{2(1 + \mu)} \quad (5)$$

$$\mu = \frac{1}{2} \frac{3K - 2G}{3K + G} \quad (6)$$

Note that if  $\mu = 0.5$  then  $K = \infty$ , the material is incompressible.

A material will undergo no volumetric strain on extension if  $\mu = 0.5$ .

For most metals  $\mu = 0.3 - 0.4$ , that is their volume increase when stretched.

For anisotropic materials the situation is much more complicated, even supposing we retain the assumption of homogeneity and elastic linearity. In the worst case twenty one independent constants must be evaluated (6), a task that is virtually impossible with a biological structure.



The situation can be improved somewhat by the assumption of orthotropicity or elastic symmetry, meaning that no shearing forces or strains are developed with a linear stress, for then only nine constants remain. In certain cases it is possible to evaluate the three tensile elastic moduli (6).

Classical elastic theory was developed from the study of deformations in metals and other hard materials and is based fundamentally on the idea that the strains observed are extremely small (infinitesimal). In the case of finite or large strains, as is often encountered in biological tissues, the postulate is no longer applicable and an entirely different mathematical technique must be introduced (6, 13). Soft body tissues deform by relatively enormous amounts, for example, strains of 2-4 as compared to 0.002 or less for metals (6). This property puts body tissues in the same class as elastomers(6).

Perhaps this is a convenient point to define the terms "stress" and "strain" as used in this report. The term stress used here is the ratio of the applied force (in grams) to the original cross-sectional area (in  $\text{mm}^2$ ) of the tissue sample in the unstressed state and it is expressed in  $\text{gm}/\text{mm}^2$ . The variation in cross-sectional area with elongation has not been taken into account. The term "strain" has been loosely used by previous workers. Lake (24) and Missirlis (30) drew typical "stress vs. extension ratio" curves in their theses but referred to them as "stress-strain" curves. In these theses extension ratio ( $\lambda$ ) was defined as the ratio of the deformed length of tissue to the original unstressed length, i.e.

$$\lambda = \frac{l_0 + \Delta l}{l_0}$$



where  $\Delta l$  = incremental length, and  $l_0$  = original unstressed length. However, in this report, "Strain" is defined as the ratio of incremental length ( $\Delta l$ ) to the original unstressed length of the tissue sample ( $l_0$ ) i.e.  $\epsilon = \Delta l / l_0$ . This should have been more accurately termed "relative deformation" or "relative elongation". The original unstressed length of the tissue sample is measured optically without taking into account the effect of "necking" due to the grips of the tensile machine.

"Necking" is considered negligible since  $l_0$  is usually at least 10 mm long. The Young's modulus of the tissue is taken to be the slope of the tangent to the stress strain curve at a specified strain.

The following paragraphs discuss the work of Fung (13) in which he tried to eliminate the vagueness and uncertainty which prevail as a result of previous workers using the infinitesimal theory of elasticity to biological materials which exhibit finite deformation.

The objective of Fung's (13) work is to discuss the non-linear stress-strain-history relationship in large deformations of living tissues. The word "history" is added to signify the dependence of stress on the history of strain, as is usually the case for biological materials. He showed that for the mesentery the most important parameter is the slope of the  $dT/d\lambda$  vs.  $T$  curve at the origin, where  $T$  stands for stress (specifically, the "Lagrangian" stress, obtained by dividing tensile load by the original cross-sectional area) and  $\lambda$  stands for the extension ratio (deformed length divided by the original length of the specimen). This parameter, which he designated by the symbol "a" is especially



suitable as a measure of the nonlinearity of the stress-strain law for biological materials (13).

Fung (13) further separated the stress-strain relationship for the mesentery into two parts: an elastic part and a history-dependent part. The elastic part defines a unique stress-strain relationship, i.e. the "elasticity" of the material. The history-dependent part is time dependent; it is related to the hysteresis, stress-relaxation, creep, and other nonconservative phenomena. Thus, it can be written as:

$$\sigma(t) = F[\epsilon(t)] + F'[\epsilon(t - \tau); t, \tau] \quad (7)$$

where  $\sigma(t)$  is the tensile stress at time  $t$  referred to the deformed state,  $\epsilon(t)$  is the tensile strain at time  $t$ ; whereas  $F'[\epsilon(t - \tau); t, \tau]$  is a function of the entire history of the strain,  $\epsilon(t - \tau)$ . The first elastic term  $F[\epsilon(t)]$  represents a thermodynamically reversible part of the stress-strain relationship. The second part represents a thermodynamically irreversible process. The first term states that at any instant of time  $t$  there is an elastic stress  $\sigma^*(t) = F[\epsilon(t)]$  corresponding to the strain  $\epsilon(t)$  at that instant. This correspondence is instantaneous, regardless of past history. The second term tells the influence of the past history (13).

In an infinitesimal deformation the concepts of stress and strain are well known. In a finite deformation, as is found in biological tissue, the description of these quantities has to be handled with care (13). An area of material composed of the same molecules changes with deformation. If a surface force is divided by the area in the deformed



state, and is resolved into components along a system of coordinates imbedded in the deformed state, then the stress is referred to as Eulerian (13). If the term "deformed state" in the preceding sentence is replaced by an "initial" or a "reference" state, the stress is said to be Lagrangian (13). Similarly, a strain tensor describes the change of the metric between two states, the initial and the deformed, and several definitions can be chosen. The matter is fairly complex and cannot be described without lengthy treatment (13).

A uniform extension may be described as follows. Let a fixed rectangular Cartesian system of coordinates  $(x, y, z)$  be used to define the unstrained body. We consider a deformation in which a unit cube in the unstrained body whose sides are parallel to the axes is deformed into a cuboid of dimensions  $\lambda_1, \lambda_2, \lambda_3$  parallel to the  $x, y, z$  axes, respectively. The coordinates of the particles in the strained body may be referred to a fixed Cartesian set of axes  $(\xi, \eta, \zeta)$  which coincide with the axes  $(x, y, z)$  so that:

$$\xi = \lambda_1 x, \eta = \lambda_2 y, \zeta = \lambda_3 z \quad (8)$$

For this uniform extensional deformation the strain components may be written in the matrix form (see "Theoretical Elasticity" by Green A.E., and W. Zerna, London: Oxford Univ. Press, 1954. See pg. 80 of this book and note that  $\lambda_{ij} = G_{ij} - g_{ij}$ ):

$$\begin{pmatrix} \gamma_{11} & \gamma_{12} & \gamma_{13} \\ \gamma_{21} & \gamma_{22} & \gamma_{23} \\ \gamma_{31} & \gamma_{32} & \gamma_{33} \end{pmatrix} = \begin{pmatrix} 1/2(\lambda_1^2 - 1) & 0 & 0 \\ 0 & 1/2(\lambda_2^2 - 1) & 0 \\ 0 & 0 & 1/2(\lambda_3^2 - 1) \end{pmatrix} \quad (9)$$



The volume of the unit cube becomes  $\lambda_1\lambda_2\lambda_3$  after deformation. The constancy of volume is expressed as a condition of incompressibility

$$\lambda_1\lambda_2\lambda_3 = 1 \quad (10)$$

Following the general practice in cardiovascular research, we shall consider the mesentery incompressible. Hence on specializing equation (8) to describe a simple tension, for which  $\sigma_{xx} = \text{const.}$ ,  $\sigma_{yy} = \sigma_{zz} = 0$ , we have

$$\lambda_1\lambda_2\lambda_3 = 1, \lambda_2 = \lambda_3 \quad (11)$$

so that

$$\lambda_2 = \lambda_3 = \frac{1}{\sqrt{\lambda_1}} \quad (12)$$

We shall write  $\lambda$  for  $\lambda_1$  in this case,

$$\lambda = \frac{\text{length of specimen under strain}}{\text{unstrained length}} = \frac{\ell}{\ell_0} \quad (13)$$

The corresponding tensile strain is

$$\epsilon = \gamma_{11} = \frac{1}{2}(\lambda^2 - 1) = \frac{1}{2} \left( \frac{\ell^2}{\ell_0^2} - 1 \right) \quad (14)$$

The cross sectional area of the specimen is decreased during extension by the ratio  $\lambda_2\lambda_3 = 1/\lambda$ . Hence if the area at the unstrained state is  $A_0$ , and the total tensile force is  $P$ , then the Eulerian stress in tension is



$$\sigma = \frac{P}{A} = \frac{P}{A_0} \lambda = T\lambda \quad (15)$$

Thus the simple tension can be described by a single component of stress  $\sigma$  and a single extension ratio  $\lambda$  (13).



## APPENDIX 2

The statistical significance of the Young's moduli of the various tissues before (in the native state) and after deelasination is calculated in the following manner.

As an illustration the case of the descending aorta will be considered here. First the "t" value between the native tissue modulus and the deelasinated tissue modulus will have to be calculated. This is commonly known as the "t-test" where t is defined by the relation

$$t = \frac{\bar{X}_1 - \bar{X}_2}{S \sqrt{\frac{1}{N_1} + \frac{1}{N_2}}}$$

where  $\bar{X}_1$  = mean modulus of native tissue,

$\bar{X}_2$  = mean modulus of deelasinated tissue,

$N_1$  = number of samples of native tissue,

$N_2$  = number of samples of deelasinated tissue,

and  $S$  = standard deviation

The standard deviation,  $S$  is in turn defined by

$$S = \sqrt{\frac{N_1 S_1^2 + N_2 S_2^2}{N_1 + N_2 - 2}}$$

where  $S_1$  = standard deviation of the mean modulus of the native tissue,

and  $S_2$  = standard deviation of the mean modulus of the deelasinated tissue.



After performing the "t test", the "p" values can be obtained from statistical tables, where p indicates the probability that the native tissue modulus will be different from the deelasinated tissue modulus. The level of significance is taken to be  $p = 0.9$ . Any "t" value which corresponds to a "p" value of less than 0.9 is considered insignificant.

Descending Aorta

Low Strain Moduli ( $\epsilon=0.2^*$ )

Number of Samples	Direction of Stress	$E_{avg.}$ (gm/mm <sup>2</sup> )		t	p
		Native	Deelasinated		
5	Circumferential	12.33 (2.15) <sup>x</sup>	10.22 (3.91)	0.94	n.s. <sup>†</sup>
5	Longitudinal	18.55 (4.20)	10.76 (3.84)	2.74	0.975

High Strain Moduli

5	Circumferential	737.8( $\epsilon=0.5^*$ ) (67.39)	790.22( $\epsilon=0.65$ ) (46.58)	1.28	n.s.
5	Longitudinal	353.9( $\epsilon=0.5$ ) (63.57)	327.7( $\epsilon=0.55$ ) (54.86)	0.624	n.s.

\* $\epsilon$  = value of strain at which modulus is calculated

x Figures in paranthesis indicate standard deviation in groups

† n.s. = not significant

TABLE 8: Determination of "t" and "p" Values for the Dog's Descending Aorta